NACA TN No. 1660

NATIONAL ADVISORY COMMITTEE FOR AERONAUTICS

TECHNICAL NOTE

No. 1660

CHARACTERISTICS OF THIN TRIANGULAR WINGS WITH CONSTANT-CHORD PARTIAL-SPAN CONTROL SURFACES AT SUPERSONIC SPEEDS

By Warren A. Tucker and Robert L. Nelson

Langley Aeronautical Laboratory
Langley Field, Va.

Washington
July 1948

NATIONAL ADVISORY COMMITTEE FOR AERONAUTICS

TECHNICAL NOTE NO. 1660

CHARACTERISTICS OF THIN TRIANGULAR WINGS WITH CONSTANT-CHORD PARTIAL-SPAN CONTROL SURFACES AT SUPERSONIC SPEEDS

By Warren A. Tucker and Robert L. Nelson

SUMMARY

A theoretical analysis was made of the characteristics of constant-chord partial-span control surfaces on thin triangular wings at supersonic speeds by use of methods based on the linearized theory for supersonic flow. Two cases were treated: In one the flap was considered to extend outboard from the center of the wing and in the other the flap was considered to extend inboard from the wing tip. Expressions were found for the lift coefficient, rolling-moment coefficient, and hinge-moment coefficient due to flap deflection, the hinge-moment coefficient due to angle of attack, and the pitching-moment coefficient due to flap lift.

A few figures are given to illustrate the application of the equations.

INTRODUCTION

The problem of the constant-chord full-span control surface on a triangular wing has been considered in reference 1. The present paper treats two types of constant-chord partial-span flaps, one extending outboard from the center of the wing and the other extending inboard from the tip of the wing (see fig. 1). The second type thus includes the flap of reference 1 as a special case. The essential parts of the solution for the outboard flaps have also been given in reference 2.

The purpose of the present paper is not to present voluminous design charts but rather to develop equations from which any of the characteristics of constant-chord partial-span flaps on triangular wings can be calculated. A few figures are given, however, which show typical variations of control-surface characteristics with ratio of flap span to wing span and with Mach number.

The analysis was made by use of methods based on the linearized equation for supersonic flow; therefore, the results are subject to

all the limitations of the linearized theory. Boundary-layer effects have been neglected.

SYMBOLS

b	maximum wing span
b_f	total flap span (see fig. 1)
c	wing root chord
c_l	wing local chord
$\bar{c}$	wing mean aerodynamic chord $\left(\frac{2}{S}\int_0^{b/2} c_l^2\, dy = \frac{2}{3}c\right)$
c_f	flap chord
$\bar{c}_f$	flap root-mean-square chord
C_L	lift coefficient $\left(\frac{L}{qS}\right)$
C_m	pitching-moment coefficient about wing mean aerodynamic center $\left(\frac{M}{qS\bar{c}}\right)$
C_l	rolling-moment coefficient $\left(\frac{l}{qSb}\right)$
C_h	hinge-moment coefficient $\left(\frac{H}{qb_f\bar{c}_f^2}\right)$
C_p	lifting pressure coefficient $\left(\frac{P}{q}\right)$
$E\left(\sqrt{1 - m^2}\right)$	complete elliptic integral of second kind with modulus $\sqrt{1 - m^2}$ (table I, equation 6)
H	hinge moment of two flaps
$k \equiv \cot \epsilon$	

L	lift of two flaps
l	rolling moment of two flaps, each deflected an amount δ in opposite directions
M	free-stream Mach number; pitching moment of two flaps about wing aerodynamic center $\left(\text{at } \frac{2}{3}c\right)$
$m \equiv \frac{\tan \epsilon}{\tan \mu}$	
P	lifting pressure
q	free-stream dynamic pressure $\left(\frac{\rho V^2}{2}\right)$
S	wing area
S_f	area of two flaps
$t \equiv \frac{y}{x \tan \epsilon}$	
V	free-stream velocity
w	vertical disturbance velocity (δV)
x,y	Cartesian coordinates parallel and normal, respectively, to free-stream direction (for field points)
ξ,η	Cartesian coordinates parallel and normal to free-stream direction (for source points)
α	angle of attack
$\beta \equiv \sqrt{M^2 - 1}$	
δ	angle of flap deflection
ϵ	wing-semiapex angle
$\zeta \equiv \tan^{-1} \frac{y}{x}$	
μ	Mach angle $\left(\tan^{-1} \frac{1}{\beta}\right)$

$\nu \equiv \frac{\beta y}{x} \equiv \frac{y/x}{\tan \mu}$

ρ free-stream density

ϕ disturbance-velocity potential

ϕ_x disturbance velocity in x-direction

Subscripts:

α partial derivative of coefficient with respect to α $\left(\text{example: } C_{h_\alpha} \equiv \frac{\partial C_h}{\partial \alpha}\right)$

δ partial derivative of coefficient with respect to δ

C_L partial derivative of coefficient with respect to C_L

∞ infinite-span or two-dimensional wing condition

All angles are in radians, unless otherwise specified.

ANALYSIS

The following analysis is concerned with constant-chord partial-span control surfaces located either outboard or inboard on the wing. (See fig. 1.) The Mach lines may be either ahead of or behind the leading edge of the wing. Because the pressure distributions for certain parts of the inboard and outboard flaps are identical, the two cases are considered concurrently.

The control-surface characteristics to be determined are as follows:

C_{L_δ} lift coefficient due to flap deflection

C_{l_δ} rolling-moment coefficient due to flap deflection

$C_{m_{C_L}}$ pitching-moment coefficient due to flap lift

C_{h_δ} hinge-moment coefficient due to flap deflection

C_{h_α} hinge-moment coefficient due to wing angle of attack

Pressure distributions.- Any of the aforementioned control-surface characteristics can be found if the pressure distributions due to flap deflection at constant angle of attack and due to angle of attack at constant flap deflection are known. This fact is true because of the principle of superposition.

The pressure distributions over certain regions of the flaps and over the wings are already known. For both the inboard flaps and the outboard flaps, the pressure due to flap deflection in the region between the Mach cones springing from the inner and outer corners of the flap is equal to the pressure on an infinite-span wing at an angle of attack. The pressure due to flap deflection in the tip Mach cone of the outboard flap when the Mach lines are ahead of the leading edge has been found in reference 1. The pressure distributions over the wing due to angle of attack have been found in reference 3 (Mach lines behind the leading edge) and reference 4 (Mach lines ahead of the leading edge).

There remain to be determined only the pressure distributions due to flap deflection in the following regions: First, the inner Mach cone of the outboard flap and the inner and outer Mach cones of the inboard flap (all three cases are identical); and, second, the tip of the outboard flap when the Mach lines are behind the leading edge. The pressure distribution for the first case is given in appendix A and for the second case, in appendix B.

The various pressure distributions are shown graphically in figures 2 and 3; the equations for the pressure distributions are given directly on the figures for ease of reference.

Derivation of control-surface characteristics.- Once the pressure distributions are known, the various control-surface characteristics can be found by integrating the pressure over the proper areas, multiplying by appropriate center-of-pressure distances when necessary, and dividing by the proper dimensions to form coefficients. Various illustrations of this procedure can be found in references 1 and 5. Giving all the derivations for the cases treated in the present paper would cause the paper to be unduly lengthy; therefore, only one sample derivation is given.

The example chosen is C_{h_δ} for the outboard flap when the Mach lines are ahead of the leading edge. The equations for the pressure distribution are found from figure 2. Consider first the inner Mach cone. Integrating the pressure only over the part of the flap contained in the Mach cone (since the pressure on the wing contributes no hinge moment) gives for the lift on this part of the flap

$$\frac{L}{q\delta} = \frac{2c_f^2}{\beta^2}\left(\frac{\pi - 1}{\pi}\right)$$

and, since the pressure distribution in the Mach cone is conical, the center of pressure of this lift is $\frac{2}{3}c_f$ behind the hinge line. The hinge moment on this part of the flap is then

$$\frac{H}{q\delta} = -\frac{2}{3}c_f\frac{2c_f^2}{\beta^2}\left(\frac{\pi - 1}{\pi}\right) = -\frac{4}{3}\frac{c_f^3}{\beta^2}\left(\frac{\pi - 1}{\pi}\right)$$

Next, for the part of the flap contained between the inner and outer Mach cones, the pressure over this entire region is noted to be constant at the two-dimensional value, so that the hinge moment can be found simply by multiplying the pressure by the moment of the trapezoidal area about the hinge line which gives

$$\frac{H}{q\delta} = \frac{6m + 8}{3}\frac{c_f^3}{\beta^2} - b_f\frac{c_f^2}{\beta}$$

The lift in the tip region has been found in reference 1 to be

$$\frac{L}{q\delta} = \frac{c_f^2}{\beta^2}(3m + 1)$$

and, since the flow in the tip region is conical, the hinge moment is

$$\frac{H}{q\delta} = -\frac{2}{3}c_f\frac{c_f^2}{\beta^2}(3m + 1) = -\frac{2}{3}\frac{c_f^3}{\beta^2}(3m + 1)$$

Adding the three hinge moments gives the total hinge moment

$$\frac{H}{q\delta} = -b_f\frac{c_f^2}{\beta} + \frac{2\pi + 4}{3\pi}\frac{c_f^3}{\beta^2}$$

The hinge-moment coefficient is formed by dividing the total hinge moment by $b_f\bar{c}_f^2/2$, which in this case is found to be

$$\frac{b_f\bar{c}_f^2}{2} = \frac{b_f c_f^2}{2} - \frac{2}{3}m\frac{c_f^3}{\beta}$$

Performing the division yields

$$C_{h_\delta}\frac{\beta}{2} = -\frac{3\frac{b_f}{b} - \frac{1}{m}\frac{\pi+2}{\pi}\frac{c_f}{c}}{3\frac{b_f}{b} - 2\frac{c_f}{c}}$$

The other control-surface characteristics may be derived in a similar manner. Before giving the final equations, however, a short discussion of the range of applicability is advisable.

Range of applicability.- Both in the discussion of pressure distributions and in the sample derivation of one of the control-surface characteristics, the Mach lines were tacitly assumed to have had the positions shown in figure 2. Many other cases are possible; for example, two Mach lines may intersect or a Mach line from one corner of a flap may cross the leading edge of the wing. These various cases have been examined to determine over just what range each equation is applicable. The method used to determine the range of applicability is given in appendix C. Expression of the limits as minimum and maximum values of b_f/b that could be used for given values of c_f/c and m is convenient.

Rather than attempt to describe verbally each case, reference is made to figures 5 and 6, which show graphically the limits found for each control-surface characteristic. The right-hand side of each figure is intended as a guide to the left-hand side and shows how the range of each equation can be found quickly from the left-hand side. The equation numbers on the figures refer to the equations which are given in tables I, II, and III. In order to make figures 5 and 6 more convenient to use, lines of constant flap area ratio S_f/S are included. In two cases the equations for C_{h_δ} as originally derived have been extended to cover a wider range. One of these extensions is derived in appendix D.

DISCUSSION AND CONCLUDING REMARKS

The final equations for the control-surface characteristics are presented in tables I, II, and III, together with the range of applicability of each equation. The equation numbers correspond to those given in figures 5 and 6.

In figure 7 are shown the variations with ratio of flap span to wing span of some of the control-surface characteristics for both inboard and outboard flaps. These calculations were made for a constant ratio of flap area to wing area of 0.2 at a value of $m = 0.8$. One point to notice is that small-chord, large-span flaps are the most efficient when the lift per unit hinge moment $-cL/H$ is used as a criterion. This general finding is consistent with the results of subsonic investigations.

The curves of $C_{l_\delta}\beta$ for outboard flaps in figure 7 show the interesting fact that for a given flap area ratio an optimum flap span ratio exists that gives the greatest rolling-moment effectiveness. This optimum flap span ratio has been found by differentiation of equations (2) and (8) and is shown in figure 8 for various values of m. For $m > 1$ (Mach lines behind the leading edge) the resultant flap is a triangular-tip control rotating about an axis normal to the stream, as shown by the small sketch on figure 8.

The variation with Mach number of the various control-surface characteristics is shown in figures 9 and 10 for two particular configurations. The equations presented in this paper can be used to calculate similar curves for other configurations.

Langley Aeronautical Laboratory
National Advisory Committee for Aeronautics
Langley Field, Va., March 31, 1948

APPENDIX A

PRESSURE DISTRIBUTION OVER INBOARD CORNER OF FLAP

The flap in figure 11 may be represented by a uniform distribution of sources and sinks. If the chordwise gap between wing and flap is considered sealed, the pressure distribution due to flap deflection may be determined by the method of reference 3.

The equation for the surface velocity potential at point (x,y) due to a uniform source distribution is given by reference 3 as

$$\phi(x,y) = -\frac{1}{\pi}\iint \frac{w\, d\xi\, d\eta}{\sqrt{(x-\xi)^2 - \beta^2(y-\eta)^2}}$$

where w is the vertical velocity and the area of integration is over the fore-cone of (x,y). Thus,

$$\phi(x,y) = -\frac{w}{\pi}\int_0^{y_1} d\eta \int_0^{x-\beta(\eta-y)} \frac{d\xi}{\sqrt{(x-\xi)^2 - \beta^2(y-\eta)^2}}$$

The first integration (reference 6, equation 260.01) gives

$$\phi(x,y) = -\frac{w}{\pi}\int_0^{y_1} d\eta \left[-\cosh^{-1}\left|\frac{x-\xi}{\beta(y-\eta)}\right| \right]_0^{x-\beta(\eta-y)}$$

$$= -\frac{w}{\pi}\int_0^{y_1} \cosh^{-1}\frac{x}{\beta|\eta-y|}\, d\eta$$

Differentiation under the integral sign with respect to x results in

$$\phi_x(x,y) = -\frac{w}{\pi}\int_0^{y_1} \frac{d\eta}{\sqrt{x^2 - \beta^2(\eta - y)^2}}$$

$$= -\frac{w}{\pi}\int_0^{y_1} \frac{d\eta}{\sqrt{x^2 - \beta^2 y + 2\beta^2 y\eta - \beta^2\eta^2}}$$

This integral can be evaluated (reference 6, equation 380.001) to give

$$\phi_x(x,y) = -\frac{w}{\pi}\left[-\frac{1}{\beta}\sin^{-1}\frac{2\beta^2 y - 2\beta^2\eta}{2\beta x}\right]_0^{y_1}$$

where at y_1

$$\eta = \frac{x + \beta y}{\beta}$$

Thus,

$$\phi_x(x,y) = -\frac{w}{\pi\beta}\left[-\sin^{-1}\frac{\beta y - (x + \beta y)}{x} + \sin^{-1}\frac{\beta y}{x}\right]$$

$$= -\frac{w}{\pi\beta}\left(\frac{\pi}{2} + \sin^{-1}\frac{\beta y}{x}\right)$$

Since ϕ_x is constant along lines $\frac{y}{x}$ = constant, a new variable $\nu = \frac{\beta y}{x}$ is introduced.

Then,

$$\phi_x(x,y) = -\frac{w}{\pi\beta}\left(\frac{\pi}{2} + \sin^{-1}\nu\right)$$

or

$$\phi_x(x,y) = -\frac{w}{\pi\beta}\cos^{-1}(-\nu)$$

From reference 3 (taking into account upper and lower surfaces),

$$C_p = -\frac{4\phi_x}{V}$$

$$C_p = \frac{4}{\pi\beta}\frac{w}{V}\left(\frac{\pi}{2} + \sin^{-1}\nu\right)$$

Since $\frac{w}{V} = \delta$,

$$C_p = \frac{4\delta}{\pi\beta}\left(\frac{\pi}{2} + \sin^{-1}\nu\right)$$

$$C_p = \frac{4\delta}{\pi\beta}\cos^{-1}(-\nu)$$

APPENDIX B

PRESSURE ON OUTER CORNER OF OUTBOARD FLAPS ($m > 1$)

The pressure within the Mach cone over the outboard corner of the flap when the Mach line lies behind the leading edge of the flap (see fig. 11) may be determined in a manner similar to that of appendix A. The equation for the potential is then the two-dimensional value $-\frac{wx}{\beta}$ minus the contribution from the source distribution in area A. Then,

$$\phi(x,y) = -\frac{wx}{\beta} + \frac{w}{\pi}\int_0^{y_1} d\eta \int_0^{k\eta} \frac{d\xi}{\sqrt{(x-\xi)^2 - \beta^2(y-\eta)^2}}$$

$$+ \frac{w}{\pi}\int_{y_1}^{y_2} d\eta \int_0^{x-\beta(\eta-y)} \frac{d\xi}{\sqrt{(x-\xi)^2 - \beta^2(y-\eta)^2}}$$

The first integration (reference 6, equation 260.01) gives

$$\phi(x,y) = -\frac{wx}{\beta} + \frac{w}{\pi}\int_0^{y_1} d\eta \left[-\cosh^{-1}\left|\frac{x-\xi}{\beta(y-\eta)}\right| \right]_0^{k\eta}$$

$$+ \frac{w}{\pi}\int_{y_1}^{y_2} d\eta \left[\cosh^{-1}\left|\frac{x-\xi}{\beta(y-\eta)}\right| \right]_0^{x-\beta(\eta-y)}$$

$$= -\frac{wx}{\beta} + \frac{w}{\pi}\int_0^{y_1} \cosh^{-1}\left|\frac{x}{\beta(y-\eta)}\right| d\eta - \frac{w}{\pi}\int_0^{y_1} \cosh^{-1}\left|\frac{x-k\eta}{\beta(y-\eta)}\right| d\eta$$

$$+ \frac{w}{\pi}\int_{y_1}^{y_2} \cosh^{-1}\left|\frac{x}{\beta(y-\eta)}\right| d\eta$$

$$= -\frac{wx}{\beta} + \frac{w}{\pi}\int_0^{y_2} \cosh^{-1}\left|\frac{x}{\beta(y-\eta)}\right| d\eta - \frac{w}{\pi}\int_0^{y_1} \cosh^{-1}\left|\frac{x-k\eta}{\beta(y-\eta)}\right| d\eta$$

Differentiation with respect to x to obtain ϕ_x gives

$$\phi_x(x,y) = -\frac{w}{\beta} + \frac{w}{\pi}\int_0^{y_2} \frac{d\eta}{\sqrt{x^2 - \beta^2(y-\eta)^2}} - \frac{w}{\pi}\int_0^{y_1} \frac{d\eta}{\sqrt{(x-k\eta)^2 - \beta^2(y-\eta)^2}}$$

$$= -\frac{w}{\beta} + \frac{w}{\pi}\int_0^{y_2} \frac{d\eta}{\sqrt{x^2 - \beta^2y^2 + 2\beta^2y\eta - \beta^2\eta^2}}$$

$$-\frac{w}{\pi}\int_0^{y_1} \frac{d\eta}{\sqrt{x^2 - \beta^2y^2 + 2(\beta^2y - kx)\eta - (\beta^2 - k^2)\eta^2}}$$

The integrals can be evaluated (reference 6, equation 380.001) to give

$$\phi_x(x,y) = -\frac{w}{\beta} + \frac{w}{\pi}\left[-\frac{1}{\beta}\sin^{-1}\frac{\beta y - \beta\eta}{x}\right]_0^{x+\beta y}$$

$$-\frac{w}{\pi}\left[-\frac{1}{\sqrt{\beta^2 - k^2}}\sin^{-1}\frac{\beta^2y - kx - (\beta^2 - k^2)\eta}{\beta(x - ky)}\right]_0^{\frac{x+\beta y}{\beta+k}}$$

$$= -\frac{w}{\beta} + \frac{w}{\pi\beta}\left(\frac{\pi}{2} + \sin^{-1}\frac{\beta y}{x}\right)$$

$$-\frac{w}{\pi\sqrt{\beta^2 - k^2}}\left[\frac{\pi}{2} - \sin^{-1}\frac{kx - \beta^2y}{\beta(x - ky)}\right]$$

$$= -\frac{w}{\pi\beta}\left(\pi - \frac{\pi}{2} - \sin^{-1}\frac{\beta y}{x}\right)$$

$$-\frac{w}{\pi\sqrt{\beta^2 - k^2}}\cos^{-1}\frac{kx - \beta^2y}{\beta(x - ky)}$$

$$= -\frac{w}{\pi\beta}\cos^{-1}\frac{\beta y}{x} - \frac{w}{\pi\beta\sqrt{1 - \frac{k^2}{\beta^2}}}\cos^{-1}\frac{k\left(1 - \frac{\beta^2y}{kx}\right)}{\beta\left(1 - \frac{k\beta y}{\beta x}\right)}$$

Let $\nu = \frac{\beta y}{x}$ and $m = \frac{\beta}{k}$; then,

$$\phi_x(x,y) = -\frac{w}{\pi\beta}\left[\cos^{-1}\nu + \frac{m}{\sqrt{m^2 - 1}}\cos^{-1}\left(\frac{1 - m\nu}{m - \nu}\right)\right]$$

Since $C_p = -\frac{4\phi_x}{V}$ and $w = \delta V$,

$$C_p = \frac{4\delta}{\pi\beta}\left[\cos^{-1}\nu + \frac{m}{\sqrt{m^2 - 1}}\cos^{-1}\left(\frac{1 - m\nu}{m - \nu}\right)\right]$$

When $\nu = 1$, this expression for C_p becomes

$$C_p = \frac{4m}{\beta\sqrt{m^2 - 1}}$$

The pressure is constant at this value everywhere outboard of the Mach cone.

APPENDIX C

METHOD OF DETERMINING THE RANGE OF APPLICABILITY

As an illustrative example, consider an outboard flap with the Mach lines ahead of the leading edge and suppose that two Mach lines cross on the flap. (See fig. 4.) It is to be determined if the equation for the lift due to flap deflection (to take a simple example) is the same equation that would be obtained if the Mach lines did not cross. The test may be made in the following manner.

First, determine the pressure coefficients in the various areas indicated by numbers in figure 5. In region 1

$$C_{p_1} = C_{p_\infty}$$

$$C_{p_2} = C_{p_\infty} - \Delta C_{p_2}$$

where ΔC_{p_2} is the result of the inboard tip effect so that

$$\Delta C_{p_2} = C_{p_\infty} - C_{p_2}$$

Similarly,

$$C_{p_3} = C_{p_\infty} - \Delta C_{p_3}$$

where ΔC_{p_3} is the result of the outboard tip effect so that

$$\Delta C_{p_3} = C_{p_\infty} - C_{p_3}$$

Now,

$$C_{p_4} = C_{p_\infty} - \Delta C_{p_2} - \Delta C_{p_3}$$

or

$$C_{p_4} = C_{p_2} + C_{p_3} - C_{p_\infty}$$

The lift per unit flap deflection is

$$\frac{L}{q\delta} = \frac{1}{\delta}\left(\int_{S_1} C_{p_1}\, dS + \int_{S_2} C_{p_2}\, dS + \int_{S_3} C_{p_3}\, dS + \int_{S_4} C_{p_4}\, dS\right)$$

$$\frac{L}{q\delta} = \frac{1}{\delta}\left(\int_{S_1} C_{p_\infty}\, dS + \int_{S_2} C_{p_2}\, dS + \int_{S_3} C_{p_3}\, dS + \int_{S_4} C_{p_2}\, dS + \int_{S_4} C_{p_3}\, dS - \int_{S_4} C_{p_\infty}\, dS\right)$$

$$\frac{L}{q\delta} = \frac{1}{\delta}\left(\int_{S_1-S_4} C_{p_\infty}\, dS + \int_{S_2+S_4} C_{p_2}\, dS + \int_{S_3+S_4} C_{p_3}\, dS\right)$$

Now, if the total area affected is written as

$$S_f' = S_1 + S_2 + S_3 + S_4$$

then

$$S_1 - S_4 = S_f' - (S_2 + S_4) - (S_3 + S_4)$$

The area covered by the inner Mach cone is $S_2 + S_4$ and the area covered by the outer Mach cone is $S_3 + S_4$, so that the final equation for $L/q\delta$ can be written as

$$\frac{L}{q\delta} = \frac{1}{\delta}\left[C_{p_\infty}(\text{Total area affected} - \text{Area in inner Mach cone} - \text{Area in outer Mach cone}) + \text{Lift in inner Mach cone} + \text{Lift in outer Mach cone}\right]$$

which is exactly the same equation that is used when the Mach lines do not cross.

This method is very convenient to use, since no lengthy integrations need be performed. Although a lift case was used as an example, the extension to other cases (hinge moment, rolling moment, and so forth) is not difficult.

APPENDIX D

CORRECTION OF C_{h_δ} FOR INBOARD FLAP WHEN MACH LINES MOVE OFF FLAP

Assume that the flap Mach lines do not move off the flap; the equation for the hinge moment due to flap deflection may be written as (see fig. 12(a))

$$H = -C_{p_\infty} q\left(\frac{c_f}{2}S_f - \frac{2}{3}c_f 2S_1\right) - 2\left(\frac{2}{3}c_f\right)\int_{S_1} C_{p_1} q \, dS$$

where the first two terms on the right represent the hinge moment over the center section and the remaining term is the hinge moment over the tips. When the Mach lines move off the flap, the flap areas behind the Mach lines can be seen from figure 12(a) to be no longer triangular and, therefore, the moment arm of these areas is no longer $\frac{2}{3}c_f$. The corrected equation may be written as (see fig. 12(b))

$$H = -C_{p_\infty} q\left(\frac{c_f}{2}S_f - \frac{2}{3}c_f 2S_1 + \bar{x}_1 2\,\Delta S_1\right)$$

$$- \frac{4}{3}c_f \int_{S_1} C_{p_1} q \, dS + 2\int_{\Delta S_1} C_{p_1} q\bar{x}_2 \, dS$$

$$= -C_{p_\infty} q\left(\frac{c_f}{2}S_f - \frac{2}{3}c_f 2S_1\right) - \frac{4}{3}c_f \int_{S_1} C_{p_1} q \, dS$$

$$- 2C_{p_\infty} q\bar{x}_1 \, \Delta S_1 + 2\int_{\Delta S_1} C_{p_1} q\bar{x}_2 \, dS$$

where $\bar{x}_1$ and $\bar{x}_2$ are the distances from the hinge line to the centroids of ΔS_1 and dS, respectively. When

$$\Delta H_1 = -2C_{p_\infty} q \bar{x}_1 \Delta S_1$$

and

$$\Delta H_2 = 2 \int_{\Delta S_1} C_{p_1} q \bar{x}_2 \, dS$$

$$H = H_{\text{uncorrected}} + \Delta H_1 + \Delta H_2$$

and

$$C_{h_\delta} = C_{h_{\delta_{\text{uncorrected}}}} + \Delta C_{h_{\delta_1}} + \Delta C_{h_{\delta_2}}$$

This part of the hinge moment ΔH_1 may be evaluated to give (see fig. 12(c))

$$\Delta H_1 = -C_{p_\infty} q \left[c_f - \frac{1}{3}\left(c_f - b_f\beta\right) \right] \left(c_f - b_f\beta\right) \frac{\left(c_f - b_f\beta\right)}{\beta}$$

$$= -\frac{2}{3} C_{p_\infty} q \frac{\left(c_f - b_f\beta\right)^3}{\beta} - C_{p_\infty} q b_f \beta \frac{\left(c_f - b_f\beta\right)^2}{\beta}$$

Since $C_{p_\infty} = \frac{4\delta}{\beta}$ and $\beta = \frac{m}{\tan \epsilon} = \frac{2c}{b} m$,

$$\frac{\Delta H_1}{q\delta} = -\frac{8}{3\beta} \frac{\left(c_f - 2cm\frac{b_f}{b}\right)^3}{2cm/b} - \frac{4b_f}{\beta}\left(c_f - 2cm\frac{b_f}{b}\right)^2$$

$$= -\frac{4bc^2}{3\beta m}\left(\frac{c_f}{c} - 2m\frac{b_f}{b}\right)^3 - \frac{4b_f c^2}{\beta}\left(\frac{c_f}{c} - 2m\frac{b_f}{b}\right)^2$$

Divide by $b_f\bar{c}_f^2$ to obtain the coefficient,

$$\Delta C_{h_{\delta_1}} = -\frac{4}{\beta}\left[\frac{1}{3m}\frac{\left(\frac{c_f}{c} - 2m\frac{b_f}{b}\right)^3}{\frac{b_f}{b}\left(\frac{c_f}{c}\right)^2} + \frac{\left(\frac{c_f}{c} - 2m\frac{b_f}{b}\right)^2}{\left(\frac{c_f}{c}\right)^2}\right]$$

For the evaluation of ΔH_2 determination of the quantity $\bar{x}_2\,dS$ is necessary. From figure 12(c) the following equations can be written

$$\bar{x}_2\,dS = \bar{x}_A A = \bar{x}_{A+B}(A + B) - \bar{x}_B B$$

$$= \frac{2}{3}c_f\frac{c_f}{2}\,db - \bar{x}_B\frac{b_f}{2}\,dc_f$$

When the variable $\nu = \frac{\tan\zeta}{\tan\mu}$ is introduced,

$$db = \frac{c_f}{\beta}\,d\nu$$

$$dc_f = \frac{\beta b_f}{\nu^2}\,d\nu$$

and

$$\bar{x}_B = \frac{2}{3}\frac{\beta b_f}{\nu}$$

Then,

$$\bar{x}\,dS = \frac{c_f^3}{3\beta}\,d\nu - \frac{\beta^2 b_f^3}{3\nu^3}\,d\nu$$

and since

$$C_{p_1} = \frac{4\delta}{\pi\beta}\left(\frac{\pi}{2} + \sin^{-1}\nu\right)$$

this part of the hinge moment ΔH_2 may be written as

$$\Delta H_2 = \frac{8\delta q}{\pi\beta}\int_{\nu_1}^{\nu_2}\left(\frac{\pi}{2} + \sin^{-1}\nu\right)\left(\frac{c_f{}^3}{3\beta} - \frac{\beta^2 b_f{}^3}{3\nu^3}\right)d\nu$$

$$\frac{\Delta H_2}{q\delta} = \frac{8}{\pi\beta}\left[\frac{c_f{}^3}{3\beta}\left(\frac{\pi}{2}\int_{\nu_1}^{\nu_2} d\nu + \int_{\nu_1}^{\nu_2}\sin^{-1}\nu\, d\nu\right)\right.$$

$$\left. - \frac{\beta^2 b_f{}^3}{3}\left(\frac{\pi}{2}\int_{\nu_1}^{\nu_2}\frac{d\nu}{\nu^3} + \int_{\nu_1}^{\nu_2}\frac{\sin^{-1}\nu\, d\nu}{\nu^3}\right)\right]$$

These integrals may be evaluated to give

$$\frac{\Delta H_2}{q\delta} = \frac{8}{\pi\beta}\left\{\frac{c_f{}^3}{3\beta}\left[\frac{\pi}{2}\nu + \nu \sin^{-1}\nu + \sqrt{1-\nu^2}\right]_{2m\frac{b_f/b}{c_f/c}}^{1} - \frac{\beta^2 b_f{}^3}{3}\left[\frac{\pi}{2}\left(-\frac{1}{2\nu^2}\right) - \frac{1}{2\nu^2}\sin^{-1}\nu - \frac{\sqrt{1-\nu^2}}{2\nu}\right]_{2m\frac{b_f/b}{c_f/c}}^{1}\right\}$$

$$= \frac{8}{\pi\beta}\left\{\frac{c_f{}^3}{3\beta}\left[\pi - \pi m\frac{b_f/b}{c_f/c} - 2m\frac{b_f/b}{c_f/c}\sin^{-1}2m\frac{b_f/b}{c_f/c} - \sqrt{1-4m^2\frac{(b_f/b)^2}{(c_f/c)^2}}\right] + \frac{\beta^2 b_f{}^3}{3}\left[\frac{\pi}{2} - \frac{\pi}{16m^2}\frac{(c_f/c)^2}{(b_f/b)^2} - \frac{(c_f/c)^2}{8m^2(b_f/b)^2}\sin^{-1}2m\frac{b_f/b}{c_f/c} - \frac{c_f/c}{4mb_f/b}\sqrt{1-4m^2\frac{(b_f/b)^2}{(c_f/c)^2}}\right]\right\}$$

This equation reduces to

$$\frac{\Delta H_2}{q\delta} = \frac{2}{\beta}\left\{bc^2\left[\frac{2(c_f/c)^3}{3m} + \frac{8m^2}{3}\left(\frac{b_f}{b}\right)^3 - \left(\frac{c_f}{c}\right)^2\frac{b_f}{b}\right] - \frac{2c_f{}^2 b_f}{\pi}\sin^{-1}2m\frac{b_f/b}{c_f/c} - \frac{bc^2}{3\pi}\frac{(c_f/c)^3}{m}\left[2 + 4m^2\frac{(b_f/b)^2}{(c_f/c)^2}\right]\sqrt{1-4m^2\frac{(b_f/b)^2}{(c_f/c)^2}}\right\}$$

Divide by $b_f\bar{c}_f^2$ to obtain the coefficient,

$$\Delta C_{h_{\delta_2}} = \frac{2}{\beta}\left\{\frac{2c_f/c}{3mb_f/b} + \frac{8}{3}m^2\frac{\left(b_f/b\right)^2}{\left(c_f/c\right)^2} - 1 - \frac{2}{\pi}\sin^{-1}2m\frac{b_f/b}{c_f/c}\right.$$
$$\left. - \frac{1}{3\pi}\frac{\left[2 + 4m^2\frac{\left(b_f/b\right)^2}{\left(c_f/c\right)^2}\right]}{m\frac{b_f}{b}\Big/\frac{c_f}{c}}\sqrt{1 - 4m^2\frac{\left(b_f/b\right)^2}{\left(c_f/c\right)^2}}\right\}$$

The expressions for $\Delta C_{h_{\delta_1}}$ and $\Delta C_{h_{\delta_2}}$ when combined with equation 18 (table III) result in equation 19.

REFERENCES

1. Tucker, Warren A.: Characteristics of Thin Triangular Wings with Constant-Chord Full-Span Control Surfaces at Supersonic Speeds. NACA TN No. 1601, 1948.

2. Lagerstrom, P. A., and Graham, Martha E.: Linearized Theory of Supersonic Control Surfaces. Rep. No. SM-13060, Douglas Aircraft Co., Inc., July 24, 1947.

3. Puckett, Allen E.: Supersonic Wave Drag of Thin Airfoils. Jour. Aero. Sci., vol. 13, no. 9, Sept. 1946, pp. 475-484.

4. Stewart, H. J.: The Lift of a Delta Wing at Supersonic Speeds. Quarterly Appl. Math., vol. IV, no. 3, Oct. 1946, pp. 246-254.

5. Tucker, Warren A.: Characteristics of Thin Triangular Wings with Triangular-Tip Control Surfaces at Supersonic Speeds with Mach Lines behind the Leading Edge. NACA TN No. 1600, 1948.

6. Dwight, Herbert Bristol: Tables of Integrals and Other Mathematical Data. Rev. ed., The Macmillan Co., 1947.

TABLE I.- CHARACTERISTICS OF OUTBOARD FLAPS ON TRIANGULAR WINGS

[$m < 1$, Mach lines ahead of leading edge]

Quantity	Equation number	Equation	Range	
			$\left(b_f/b\right)_{min}$	$\left(b_f/b\right)_{max}$
C_{l_δ}	1	$C_{l_\delta} = \frac{4}{\beta}\left[2\frac{b_f}{b}\frac{c_f}{c} - \frac{1+m}{2m}\left(\frac{c_f}{c}\right)^2\right]$	$\frac{1}{m}\frac{c_f}{c}$	1.0
C_{l_δ}	2	$C_{l_\delta} = \frac{2}{\beta}\left\{\left[2\frac{b_f}{b} - \left(\frac{b_f}{b}\right)^2\right]\frac{c_f}{c} - \frac{1+m}{2m}\left(\frac{c_f}{c}\right)^2 + \frac{3m^2+6m-1}{24m^2}\left(\frac{c_f}{c}\right)^3\right\}$	$\frac{1}{m}\frac{c_f}{c}$	1.0
$C_{m_{C_L}}$	3	$C_{m_{C_L}} = -\frac{1}{2}\frac{4m\frac{b_f}{b} - \left[1+\left(1+6\frac{b_f}{b}\right)m\right]\frac{c_f}{c} + (1+3m)\left(\frac{c_f}{c}\right)^2}{4m\frac{b_f}{b} - (1+m)\frac{c_f}{c}}$	$\frac{1}{m}\frac{c_f}{c}$	1.0
C_{h_δ}	4	$C_{h_\delta} = -\frac{2}{\beta}\frac{3\frac{b_f}{b} - \frac{1}{m}\frac{\pi+2}{\pi}\frac{c_f}{c}}{3\frac{b_f}{b} - 2\frac{c_f}{c}}$	$\left(1+\frac{1}{m}\right)\frac{c_f}{c}$	$1 - \frac{1}{2m}\frac{c_f}{c}$
C_{h_δ}	5	$C_{h_\delta} = -\frac{2}{\beta}\frac{3\frac{b_f}{b} - \frac{1}{m}\frac{\pi+2}{\pi}\frac{c_f}{c} + \left[\frac{2}{m\pi}\frac{c_f}{c} + \frac{4m}{\pi}\frac{\left(1-\frac{b_f}{b}\right)^2}{c_f/c}\right]\sqrt{1 - \frac{4m^2\left(1-\frac{b_f}{b}\right)^2}{c_f/c^2}} - \frac{6}{\pi}\left(1-\frac{b_f}{b}\right)\cos^{-1}\frac{2m\left(1-\frac{b_f}{b}\right)}{c_f/c}}{3\frac{b_f}{b} - 2\frac{c_f}{c}}$	$\left(1+\frac{1}{m}\right)\frac{c_f}{c}$; $\frac{c_f}{c} > \frac{2m}{1+2m}$ $\left(1-\frac{1}{2m}\right)\frac{c_f}{c}$; $\frac{c_f}{c} < \frac{2m}{1+2m}$	1.0
C_{h_α}	6	$C_{h_\alpha} = -\frac{2}{\beta}\frac{m}{E\left(\sqrt{1-m^2}\right)}\frac{1}{\left[3\frac{b_f}{b}\left(\frac{c_f}{c}\right)^2 - 2\left(\frac{c_f}{c}\right)^3\right]}\left\{\left(1-\frac{c_f}{c}\right)^3\cos^{-1}\frac{1-\frac{b_f}{b}}{1-\frac{c_f}{c}} - \left(1-3\frac{c_f}{c}\right)\cos^{-1}\left(1-\frac{b_f}{b}\right)\right.$ $\left. - \left(1-\frac{b_f}{b}\right)^3\left[\cosh^{-1}\left(\frac{1}{1-\frac{b_f}{b}}\right) - \cosh^{-1}\left(\frac{1-\frac{c_f}{c}}{1-\frac{b_f}{b}}\right)\right] + \left(2-3\frac{c_f}{c}\right)\left(1-\frac{b_f}{b}\right)\sqrt{1-\left(1-\frac{b_f}{b}\right)^2}\right.$ $\left. - 2\left(1-\frac{c_f}{c}\right)\left(1-\frac{b_f}{b}\right)\sqrt{\left(1-\frac{c_f}{c}\right)^2 - \left(1-\frac{b_f}{b}\right)^2}\right\}$	c_f/c	1.0

TABLE II.- CHARACTERISTICS OF OUTBOARD FLAPS ON TRIANGULAR WINGS

[$m > 1$, Mach lines behind leading edge]

Quantity	Equation number	Equation	Range	
			$\left(\frac{b_f}{b}\right)_{min}$	$\left(\frac{b_f}{b}\right)_{max}$
c_{l_δ}	7	$c_{l_\delta} = \frac{1}{\beta}\left[2\frac{b_f}{b}\frac{c_f}{c} - \left(\frac{c_f}{c_o}\right)^2\right]$	c_f/c_o	1.0
c_{l_δ}	8	$c_{l_\delta} = \frac{2}{\beta}\left\{\left[2\frac{b_f}{b} - \left(\frac{b_f}{b}\right)^2\right]\frac{c_f}{c_o} - \left(\frac{c_f}{c_o}\right)^2 + \frac{1}{3}\left(\frac{c_f}{c_o}\right)^3\right\}$	c_f/c_o	1.0
$c_{m_{\delta_L}}$	9	$c_{m_{\delta_L}} = -\frac{2\frac{b_f}{b} - \left(1 + 3\frac{b_f}{b}\right)\frac{c_f}{c_o} + 2\left(\frac{c_f}{c_o}\right)^2}{4\frac{b_f}{b} - 2\frac{c_f}{c_o}}$	c_f/c_o	1.0
c_{h_δ}	10	$c_{h_\delta} = -\frac{2}{\beta}\frac{3\frac{b_f}{b} - \frac{1}{m}\frac{m+1}{m}\frac{c_f}{c_o}}{3\frac{b_f}{b} - 2\frac{c_f}{c_o}}$	$\left(1 + \frac{1}{m}\right)\frac{c_f}{c_o}$	$1 - \frac{1}{2m}\frac{c_f}{c_o}$
c_{h_δ}	11	$c_{h_\delta} = -\frac{2}{\beta}\frac{3\frac{b_f}{b} - \frac{1}{m}\frac{m+1}{m}\frac{c_f}{c_o} + \left[\frac{2}{m}\frac{c_f}{c_o} + \frac{1}{m}\frac{m-1}{m}\frac{\left(1 - \frac{b_f}{b}\right)^2}{c_f/c_o}\right]\sqrt{1 - \frac{m^2\left(1 - \frac{b_f}{b}\right)^2}{\left(c_f/c_o\right)^2}} - \frac{6}{\pi}\left(1 - \frac{b_f}{b}\right)\cos^{-1}\frac{m\left(1 - \frac{b_f}{b}\right)}{c_f/c_o}}{3\frac{b_f}{b} - 2\frac{c_f}{c_o}}$	$\left(1 + \frac{1}{m}\right)\frac{c_f}{c_o}$; $\frac{c_f}{c_o} > \frac{2m}{2m+1}$ $1 - \frac{1}{2m}\frac{c_f}{c_o}$; $\frac{c_f}{c_o} < \frac{2m}{2m+1}$	1.0
$c_{h_{\dot{\alpha}}}$	12	$c_{h_{\dot{\alpha}}} = -\frac{2}{\beta}\frac{m}{\sqrt{m^2-1}}\frac{3\frac{b_f}{b} - \frac{c_f}{c_o}}{3\frac{b_f}{b} - 2\frac{c_f}{c_o}}$	c_f/c_o	$\frac{m-1}{m}$
c_{h_α}	13	$c_{h_\alpha} = -\frac{2}{\pi\beta}\frac{\pi}{3\frac{b_f}{b}\left(\frac{c_f}{c_o}\right)^2 - 2\left(\frac{c_f}{c_o}\right)^3}\left[\left(3\frac{c_f}{c} - 1\right)\cos^{-1}\left[m\left(1 - \frac{b_f}{b}\right)\right] - m\left(1 - \frac{b_f}{b}\right)^3\cosh^{-1}\frac{1}{m\left(1 - \frac{b_f}{b}\right)}\right.$ $+ \frac{m}{\sqrt{m^2-1}}\left\{\frac{\pi}{2}\left\{\left(\frac{c_f}{c_o}\right)^2\left(3 - \frac{c_f}{c_o}\right) - \left(1 - \frac{b_f}{b}\right)\left[\left(1 - \frac{b_f}{b}\right)^2 + 3\left(1 - \frac{c_f}{c_o}\right)^2\right]\right\} + \left(1 - \frac{b_f}{b}\right)\left[3\left(1 - 2\frac{c_f}{c_o}\right) + \left(1 - \frac{b_f}{b}\right)^2\right]\cos^{-1}\frac{1}{m}\sqrt{\frac{1 - m^2\left(1 - \frac{b_f}{b}\right)^2}{1 - \left(1 - \frac{b_f}{b}\right)^2}}$ $\left. + \left[3\left(1 - \frac{c_f}{c_o}\right)\left(1 - \frac{b_f}{b}\right)^2 + \left(1 - 2\frac{c_f}{c_o}\right)\right]\cos^{-1}\left(1 - \frac{b_f}{b}\right)\sqrt{\frac{m^2-1}{1 - \left(1 - \frac{b_f}{b}\right)^2}}\right\}\right]$	$\frac{c_f}{c_o}$; $\frac{c_f}{c_o} > \frac{m-1}{m}$ $\frac{m-1}{m}$; $\frac{c_f}{c_o} < \frac{m-1}{m}$	$\frac{m-1}{m} + \frac{1}{m}\frac{c_f}{c_o}$
c_{h_α}	14	$c_{h_\alpha} = -\frac{2}{\pi\beta}\frac{\pi}{3\frac{b_f}{b}\left(\frac{c_f}{c_o}\right)^2 - 2\left(\frac{c_f}{c_o}\right)^3}\left(\left(3\frac{c_f}{c_o} - 1\right)\cos^{-1}\left[m\left(1 - \frac{b_f}{b}\right)\right] + \left(1 - \frac{c_f}{c_o}\right)^3\cos^{-1}\frac{m\left(1 - \frac{b_f}{b}\right)}{1 - \frac{c_f}{c_o}} - m\left(1 - \frac{b_f}{b}\right)^3\left[\cosh^{-1}\frac{1}{m\left(1 - \frac{b_f}{b}\right)} - \cosh^{-1}\frac{1 - \frac{c_f}{c_o}}{m\left(1 - \frac{b_f}{b}\right)}\right]\right.$ $+ \frac{m}{\sqrt{m^2-1}}\left[\frac{\pi}{2}\left(\frac{c_f}{c_o}\right)^2\left(3 - \frac{c_f}{c_o}\right) + \left(1 - \frac{b_f}{b}\right)\left[3\left(1 - 2\frac{c_f}{c_o}\right) + \left(1 - \frac{b_f}{b}\right)^2\right]\cos^{-1}\frac{1}{m}\sqrt{\frac{1 - m^2\left(1 - \frac{b_f}{b}\right)^2}{1 - \left(1 - \frac{b_f}{b}\right)^2}}\right.$ $+ \left[3\left(1 - \frac{c_f}{c_o}\right)\left(1 - \frac{b_f}{b}\right)^2 + \left(1 - 2\frac{c_f}{c_o}\right)\right]\cos^{-1}\left(1 - \frac{b_f}{b}\right)\sqrt{\frac{m^2-1}{1 - \left(1 - \frac{b_f}{b}\right)^2}} - \left(1 - \frac{b_f}{b}\right)\left[3\left(1 - \frac{c_f}{c_o}\right)^2 + \left(1 - \frac{b_f}{b}\right)^2\right]\cos^{-1}\frac{1}{m}\sqrt{\frac{\left(1 - \frac{c_f}{c_o}\right)^2 - m^2\left(1 - \frac{b_f}{b}\right)^2}{\left(1 - \frac{c_f}{c_o}\right)^2 - \left(1 - \frac{b_f}{b}\right)^2}}$ $\left. - \left(1 - \frac{c_f}{c_o}\right)\left[3\left(1 - \frac{b_f}{b}\right)^2 + \left(1 - \frac{c_f}{c_o}\right)^2\right]\cos^{-1}\left(1 - \frac{b_f}{b}\right)\sqrt{\frac{m^2-1}{\left(1 - \frac{c_f}{c_o}\right)^2 - \left(1 - \frac{b_f}{b}\right)^2}}\right\}\right)$	$\frac{m-1}{m} + \frac{1}{m}\frac{c_f}{c_o}$	1.0

NACA

TABLE III.- CHARACTERISTICS OF THICKNESS FLOWS ON TRIANGULAR WINGS

[$m < 1$ or $m > 1$; Mach lines ahead of or behind leading edge]

Quantity	Equation number	Equation	Range		
			$\left(\frac{b_f}{b}\right)_{min}$	$\left(\frac{b_f}{b}\right)_{max}$	m
C_{l_D}	15	$C_{l_D} = \frac{1}{\beta}\left(\sigma\frac{b_f}{b}\frac{\sigma_f}{\sigma}\right)$	0	$1 - \frac{1}{m}\frac{\sigma_f}{\sigma}$	< 1
			0	$1 - \frac{\sigma_f}{\sigma}$	> 1
C_{l_D}	16	$C_{l_D} = \frac{1}{\beta}\left[\sigma\left(\frac{b_f}{b}\right)^2\frac{\sigma_f}{\sigma}\right]$	0	$1 - \frac{1}{m}\frac{\sigma_f}{\sigma}$	< 1
			0	$1 - \frac{\sigma_f}{\sigma}$	> 1
$C_{m_{C_L}}$	17	$C_{m_{C_L}} = -\frac{1}{\beta}\left(\frac{1}{4} - \frac{3}{8}\frac{\sigma_f}{\sigma}\right)$	0	$1 - \frac{1}{m}\frac{\sigma_f}{\sigma}$	< 1
			0	$1 - \frac{\sigma_f}{\sigma}$	> 1
C_{D_0}	18	$C_{D_0} = -\frac{\sigma}{\beta}\left(1 - \frac{2\sigma_f/\sigma}{3\tan\beta_f/b}\right)$	$\frac{1}{\beta m}\frac{\sigma_f}{\sigma}$	$1 - \frac{m+1}{\beta m}\frac{\sigma_f}{\sigma}$	< 1
			$\frac{1}{\beta m}\frac{\sigma_f}{\sigma}$	$1 - \frac{\sigma_f}{\sigma}$	> 1
C_{D_0}	19	$C_{D_0} = -\frac{\sigma}{\beta}\left[\frac{\sigma}{\pi}\sin^{-1}\frac{2\tan\beta_f/b}{c_f/c} + \frac{2\left(\frac{\sigma_f}{c}\right)^2 + m\sigma^2\left(\frac{b_f}{b}\right)^2}{3m\frac{b_f}{b}\left(\frac{\sigma_f}{\sigma}\right)^2}\sqrt{\left(\frac{\sigma_f}{c}\right)^2 - m\sigma^2\left(\frac{b_f}{b}\right)^2} - \frac{2\sigma_f/\sigma}{3\tan\beta_f/b}\right]$	0	$1 - \frac{m+1}{\beta m}\frac{\sigma_f}{\sigma}$; $\frac{\sigma_f}{\sigma} > \frac{\beta m}{m+1}$ $\frac{1}{\beta m}\frac{\sigma_f}{\sigma}$; $\frac{\sigma_f}{\sigma} < \frac{\beta m}{m+1}$	< 1
			0	$1 - \frac{\sigma_f}{\sigma}$; $\frac{\sigma_f}{\sigma} > \frac{\beta m}{1+\beta m}$ $\frac{1}{\beta m}\frac{\sigma_f}{\sigma}$; $\frac{\sigma_f}{\sigma} < \frac{\beta m}{1+\beta m}$	> 1
C_{D_M}	20	$C_{D_M} = -\frac{\sigma}{\beta}\left[\frac{m}{\sqrt{m^2-1}} + \left(1 - \frac{m}{\sqrt{m^2-1}}\right)\left(1 - \frac{1}{3}\frac{\sigma_f}{\sigma}\right)\left(\frac{b_f}{b}\right)^2\right]$	$1/m$	$1 - \frac{\sigma_f}{\sigma}$	> 1
C_{D_M}	21	$C_{D_M} = -\frac{\sigma}{\beta}\frac{\sigma}{3\pi\frac{b_f}{b}\left(\frac{\sigma_f}{\sigma}\right)^2}\left[\frac{3\pi}{8}\left(1 - \frac{\sigma_f}{\sigma}\right)^3 - \left(1 - 3\frac{\sigma_f}{\sigma}\right)\sin^{-1}\left(m\frac{b_f}{b}\right) + m\left(\frac{b_f}{b}\right)^3\cosh^{-1}\frac{1}{m\beta_f/b} - \frac{m}{\sqrt{m^2-1}}\left(\left[\left(\frac{b_f}{b}\right)^2 + 3\frac{b_f}{b}\left(1 - m\frac{\sigma_f}{\sigma}\right)\right]\cos^{-1}\frac{1}{m}\sqrt{\frac{1 - m^2\left(\frac{b_f}{b}\right)^2}{1 - \left(\frac{b_f}{b}\right)^2}}\right.\right.$ $\left.\left. + \left[3\left(\frac{b_f}{b}\right)^2\left(1 - \frac{\sigma_f}{\sigma}\right) + \left(1 - 3\frac{\sigma_f}{\sigma}\right)\right]\cos^{-1}\frac{b_f}{b}\sqrt{\frac{m^2-1}{1 - \left(\frac{b_f}{b}\right)^2}} - \frac{\pi}{8}\left\{\frac{b_f}{b}\left[3\left(1 - \frac{\sigma_f}{\sigma}\right)^2 + \left(\frac{b_f}{b}\right)^2\right] - \left(\frac{\sigma_f}{\sigma}\right)^2\left(3 - \frac{\sigma_f}{\sigma}\right)\right\}\right)\right]$	$\frac{1}{m}\left(1 - \frac{\sigma_f}{\sigma}\right)$	$1 - \frac{\sigma_f}{\sigma}$; $\frac{\sigma_f}{\sigma} > \frac{m-1}{m}$ $\frac{1}{m}\frac{\sigma_f}{\sigma} < \frac{m-1}{m}$	> 1
C_{D_M}	22	$C_{D_M} = -\frac{\sigma}{\beta}\frac{\sigma}{3\pi\frac{b_f}{b}\left(\frac{\sigma_f}{\sigma}\right)^2}\left(\left(1 - \frac{\sigma_f}{\sigma}\right)^3\sin^{-1}\frac{m\beta_f/b}{1 - \frac{\sigma_f}{\sigma}} - \left(1 - 3\frac{\sigma_f}{\sigma}\right)\sin^{-1}\left(m\frac{b_f}{b}\right) + m\left(\frac{b_f}{b}\right)^3\left(\cosh^{-1}\frac{1}{m\beta_f/b} - \cosh^{-1}\frac{1 - \frac{\sigma_f}{\sigma}}{m\beta_f/b}\right)\right.$ $+ \frac{m}{\sqrt{m^2-1}}\left\{\left[\left(\frac{b_f}{b}\right)^3 + 3\frac{b_f}{b}\left(1 - \frac{\sigma_f}{\sigma}\right)^2\right]\cos^{-1}\frac{1}{m}\sqrt{\frac{\left(1 - \frac{\sigma_f}{\sigma}\right)^2 + m^2\left(\frac{b_f}{b}\right)^2}{\left(1 - \frac{\sigma_f}{\sigma}\right)^2 - \left(\frac{b_f}{b}\right)^2}} - \left[\left(\frac{b_f}{b}\right)^3 - 3\frac{b_f}{b}\left(1 - m\frac{\sigma_f}{\sigma}\right)\right]\cos^{-1}\frac{1}{m}\sqrt{\frac{1 - m^2\left(\frac{b_f}{b}\right)^2}{1 - \left(\frac{b_f}{b}\right)^2}}\right.$ $\left.\left.\left. + \left[3\left(\frac{b_f}{b}\right)^2\left(1 - \frac{\sigma_f}{\sigma}\right) + \left(1 - 3\frac{\sigma_f}{\sigma}\right)\right]\cos^{-1}\frac{b_f}{b}\sqrt{\frac{m^2-1}{\left(1 - \frac{\sigma_f}{\sigma}\right)^2 - \left(\frac{b_f}{b}\right)^2}} - \left[3\left(\frac{b_f}{b}\right)^2\left(1 - \frac{\sigma_f}{\sigma}\right) + \left(1 - 3\frac{\sigma_f}{\sigma}\right)\right]\cos^{-1}\sqrt{\frac{m^2-1}{1 - \left(\frac{b_f}{b}\right)^2}} - \frac{\pi}{8}\left[3\left(\frac{\sigma_f}{\sigma}\right)^2 - \left(\frac{\sigma_f}{\sigma}\right)^3\right]\right\}\right)$	0	$\frac{1}{m}\left(1 - \frac{\sigma_f}{\sigma}\right)$	> 1
C_{D_0}	23	$C_{D_0} = -\frac{\sigma}{\beta}\frac{m}{\pi\left(\sqrt{1-m^2}\right)}\frac{1}{3\frac{b_f}{b}\left(\frac{\sigma_f}{\sigma}\right)^2}\left[\left(1 - \frac{\sigma_f}{\sigma}\right)^3\sin^{-1}\frac{b_f/b}{1 - \frac{\sigma_f}{c}} - \left(1 - 3\frac{\sigma_f}{\sigma}\right)\sin^{-1}\frac{b_f}{b} - \frac{b_f}{b}\left(4 - 3\frac{\sigma_f}{\sigma}\right)\sqrt{1 - \left(\frac{b_f}{b}\right)^2} + 2\frac{b_f}{b}\left(1 - \frac{\sigma_f}{\sigma}\right)\sqrt{\left(1 - \frac{\sigma_f}{\sigma}\right)^2 - \left(\frac{b_f}{b}\right)^2}\right.$ $\left. + \left(\frac{b_f}{b}\right)^3\left(\cosh^{-1}\frac{1}{b_f/b} - \cosh^{-1}\frac{1 - \frac{\sigma_f}{c}}{b_f/b}\right)\right]$	0	$1 - \frac{\sigma_f}{\sigma}$	< 1

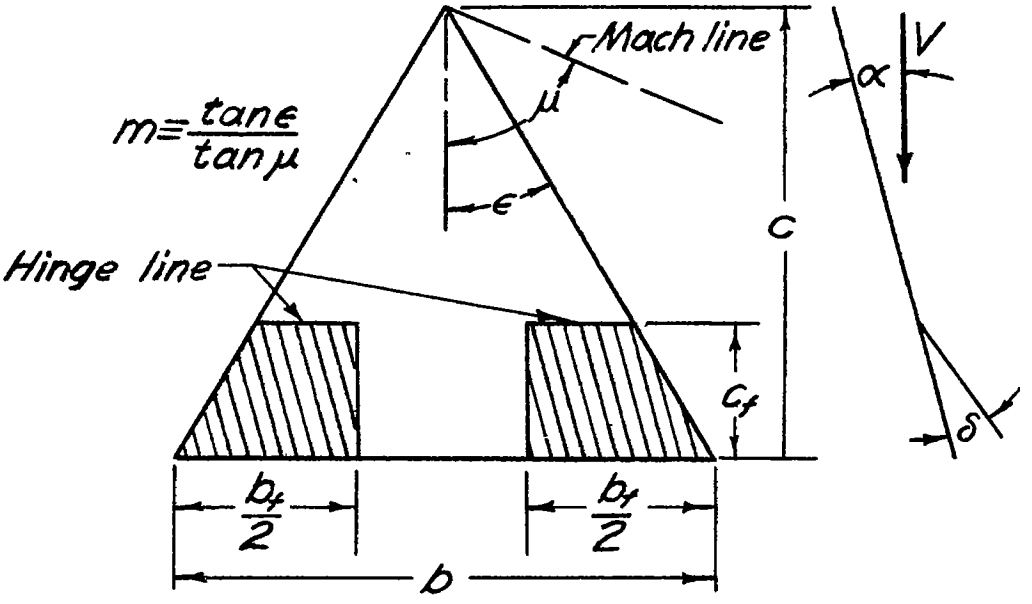

(a) Outboard flaps.

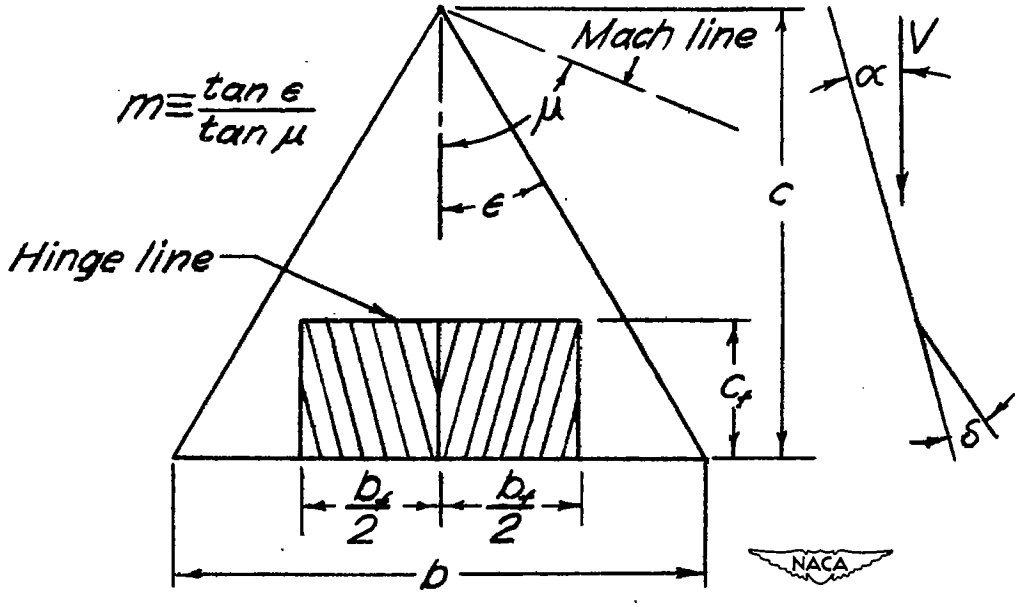

(b) Inboard flaps.

Figure 1.- Control-surface configurations.

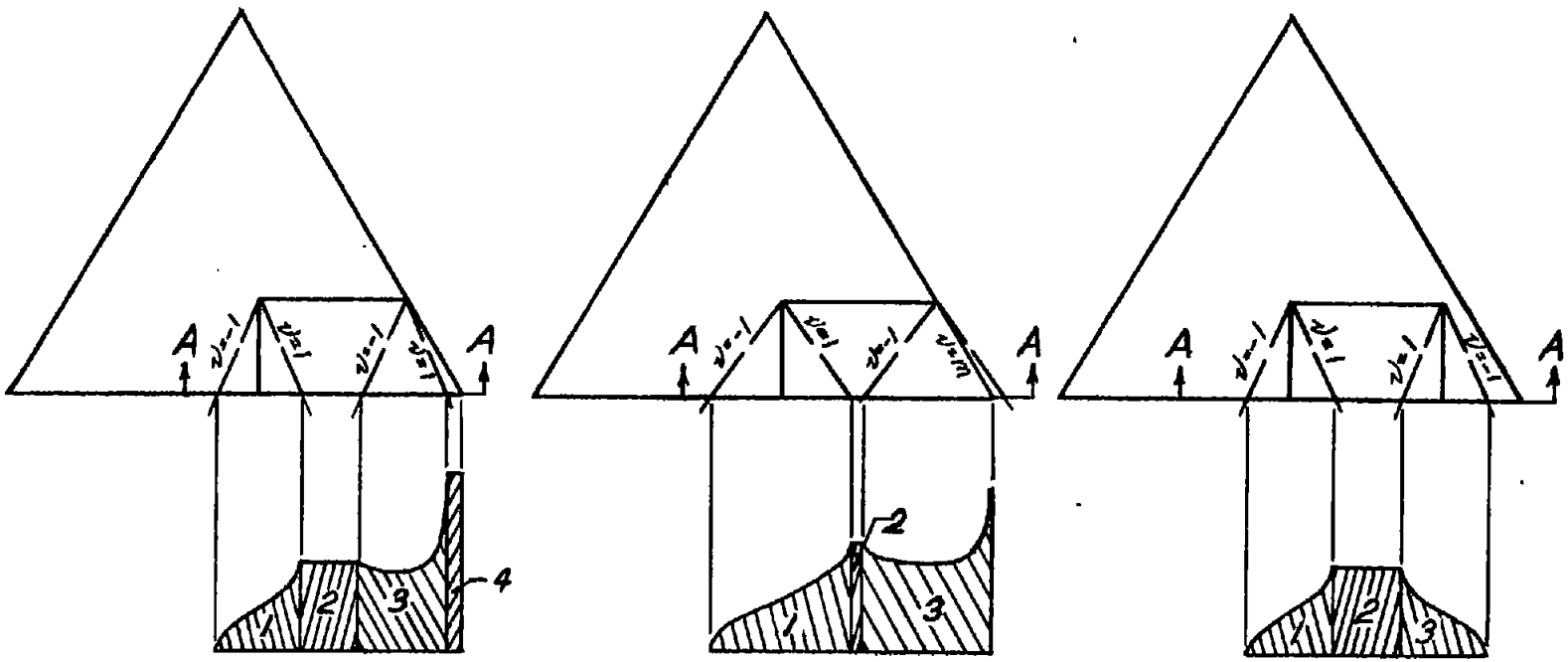

$$\frac{c_{p_1}}{\delta} = \frac{4}{\pi\beta}\cos^{-1}\nu; \quad \frac{c_{p_2}}{\delta} = \frac{4}{\beta}$$

$$\frac{c_{p_3}}{\delta} = \frac{4}{\pi\beta}\left[\cos^{-1}\nu + \frac{m}{\sqrt{m^2-1}}\cos^{-1}\left(\frac{1-m\nu}{m-\nu}\right)\right]$$

$$\frac{c_{p_4}}{\delta} = \frac{4m}{\beta\sqrt{m^2-1}}$$

(a) Outboard flap; $m > 1$.

$$\frac{c_{p_1}}{\delta} = \frac{4}{\pi\beta}\cos^{-1}\nu; \quad \frac{c_{p_2}}{\delta} = \frac{4}{\beta}$$

$$\frac{c_{p_3}}{\delta} = \frac{8}{\pi\beta}\left(\frac{m}{1+m}\sqrt{\frac{1+\nu}{m-\nu}} + \tan^{-1}\sqrt{\frac{m-\nu}{1+\nu}}\right)$$

(b) Outboard flap; $m < 1$.

$$\frac{c_{p_1}}{\delta} = \frac{4}{\pi\beta}\cos^{-1}\nu; \quad \frac{c_{p_2}}{\delta} = \frac{4}{\beta}$$

$$c_{p_3} = c_{p_1}$$

(c) Inboard flap.

Figure 2.- Pressure distributions due to flap deflection.

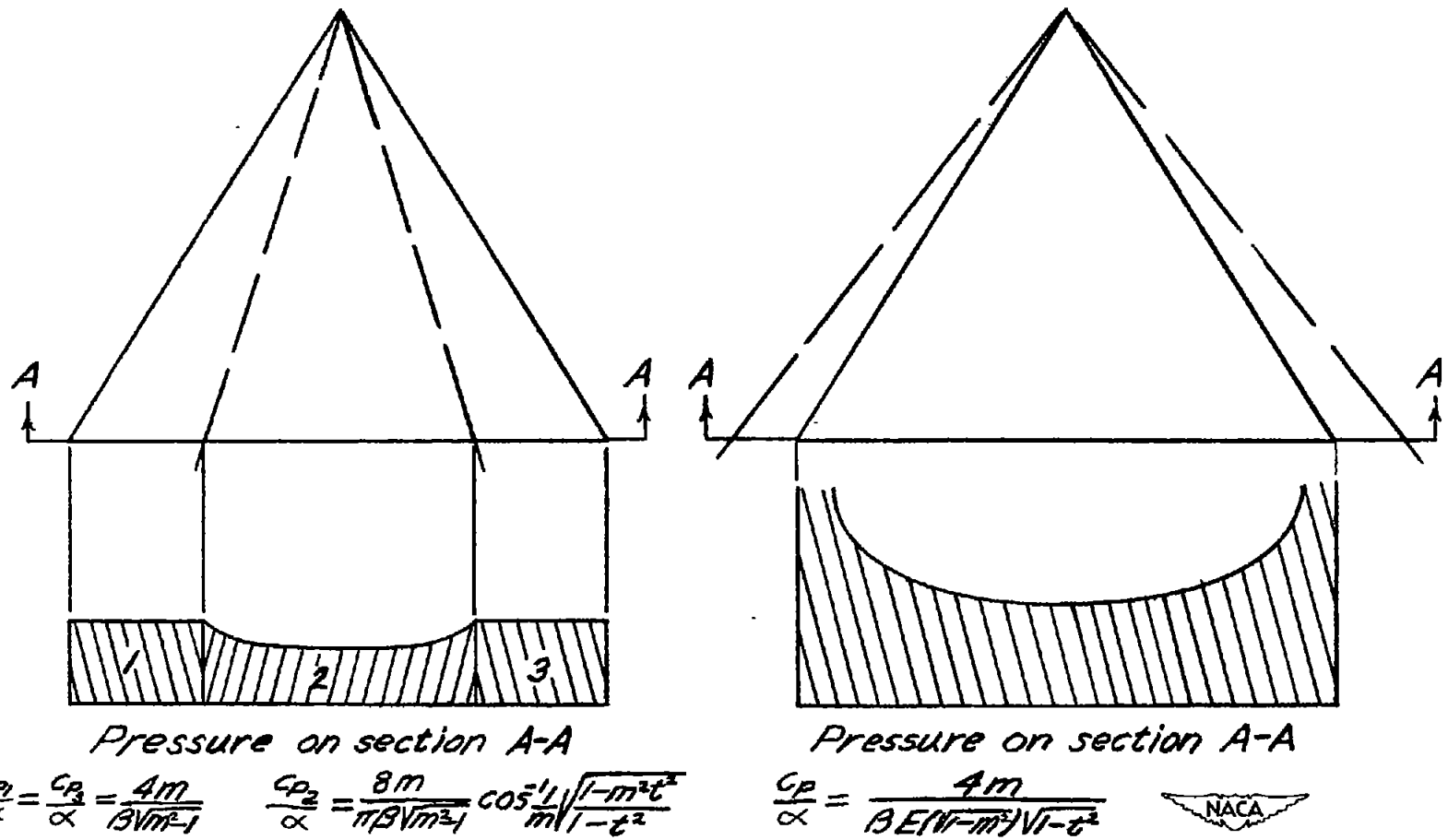

(a) m > 1 (reference 3).

(b) m < 1 (reference 4).

Figure 3.- Pressure distributions due to angle of attack.

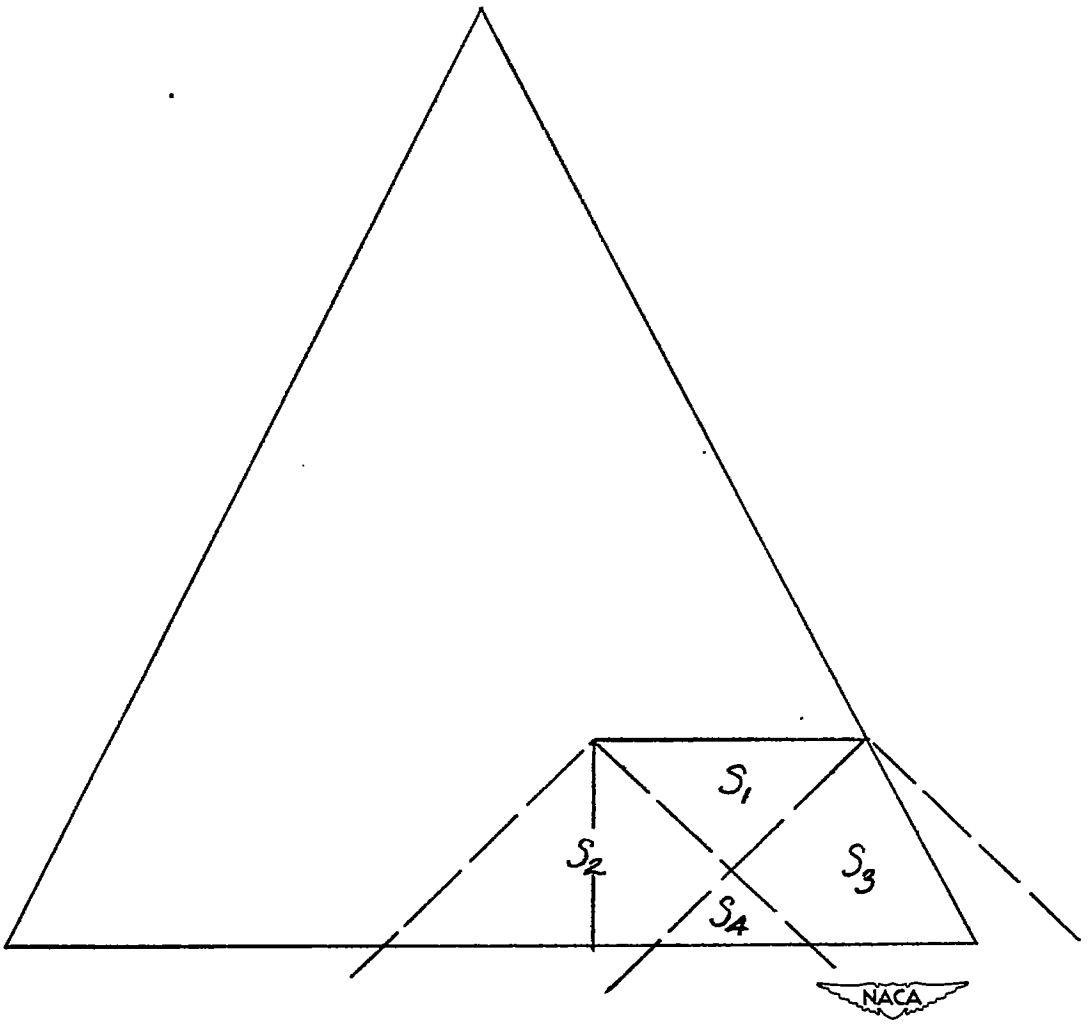

Figure 4.- Notation used in appendix C.

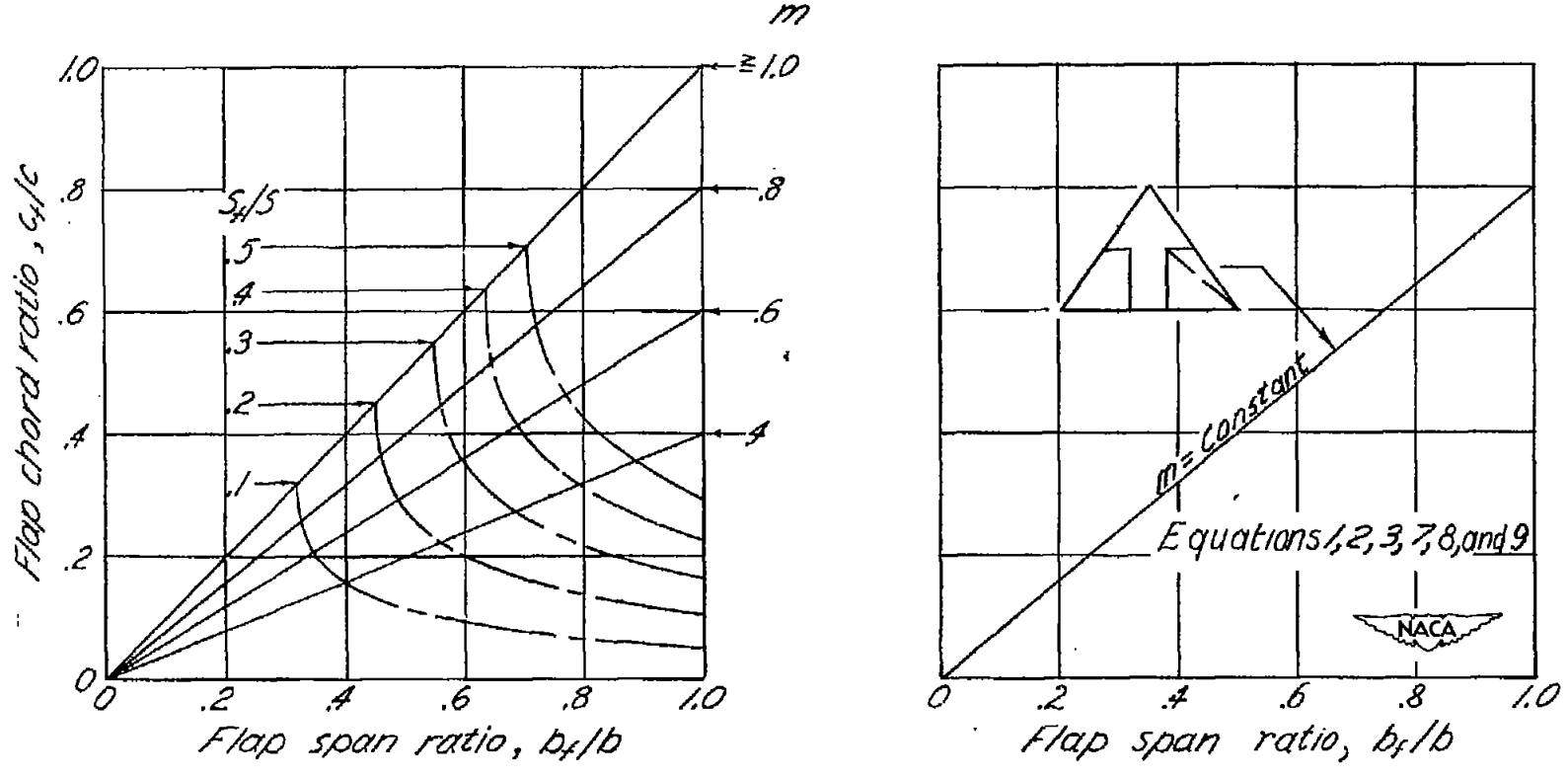

(a) C_{L_δ}, C_{l_δ}, $C_{m_{C_L}}$ (equations 1, 2, 3, 7, 8, and 9).

Figure 5.- Range of applicability of equations for outboard flaps.

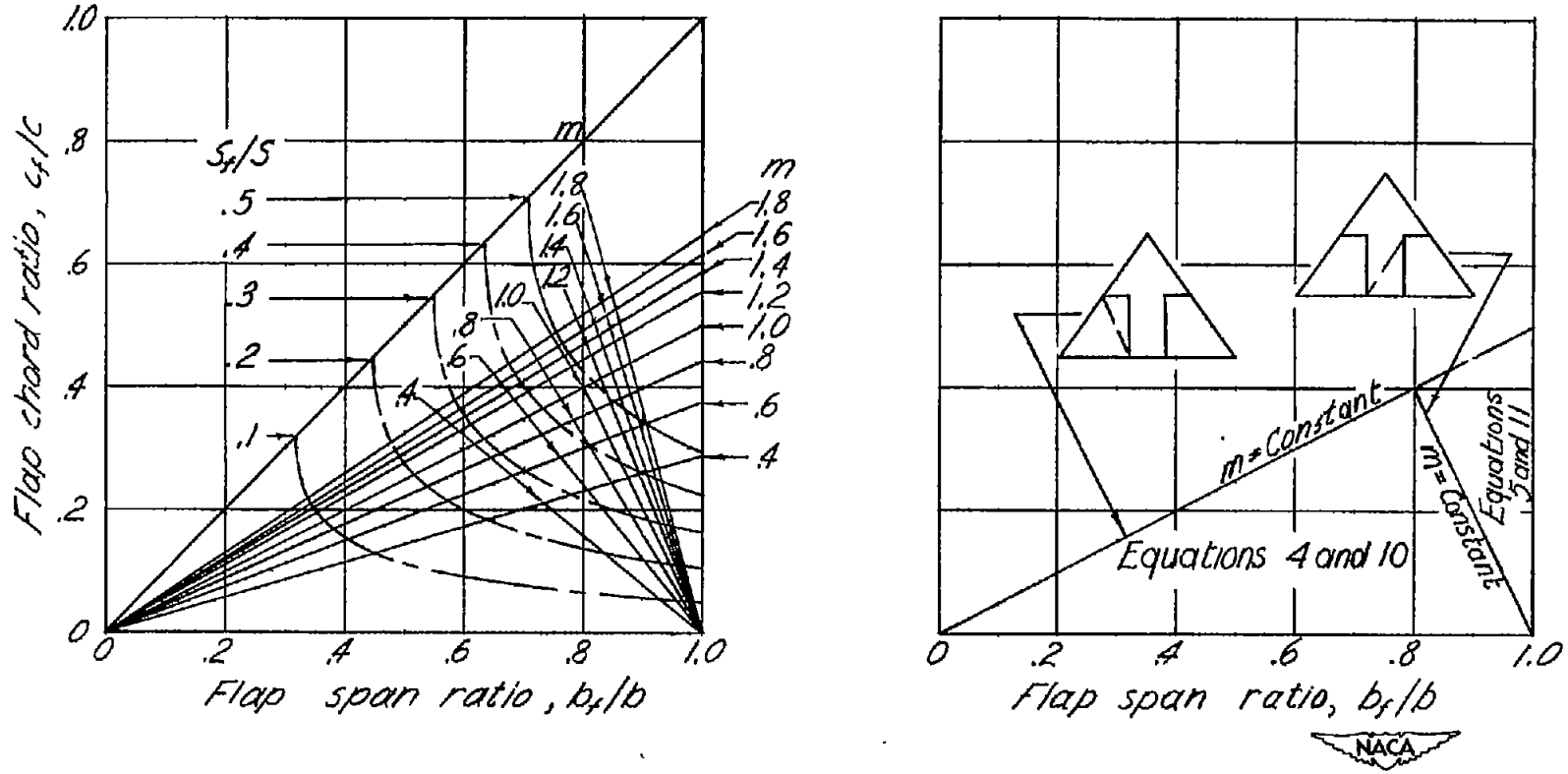

(b) C_{h_δ} (equations 4, 5, 10, and 11).

Figure 5.- Continued.

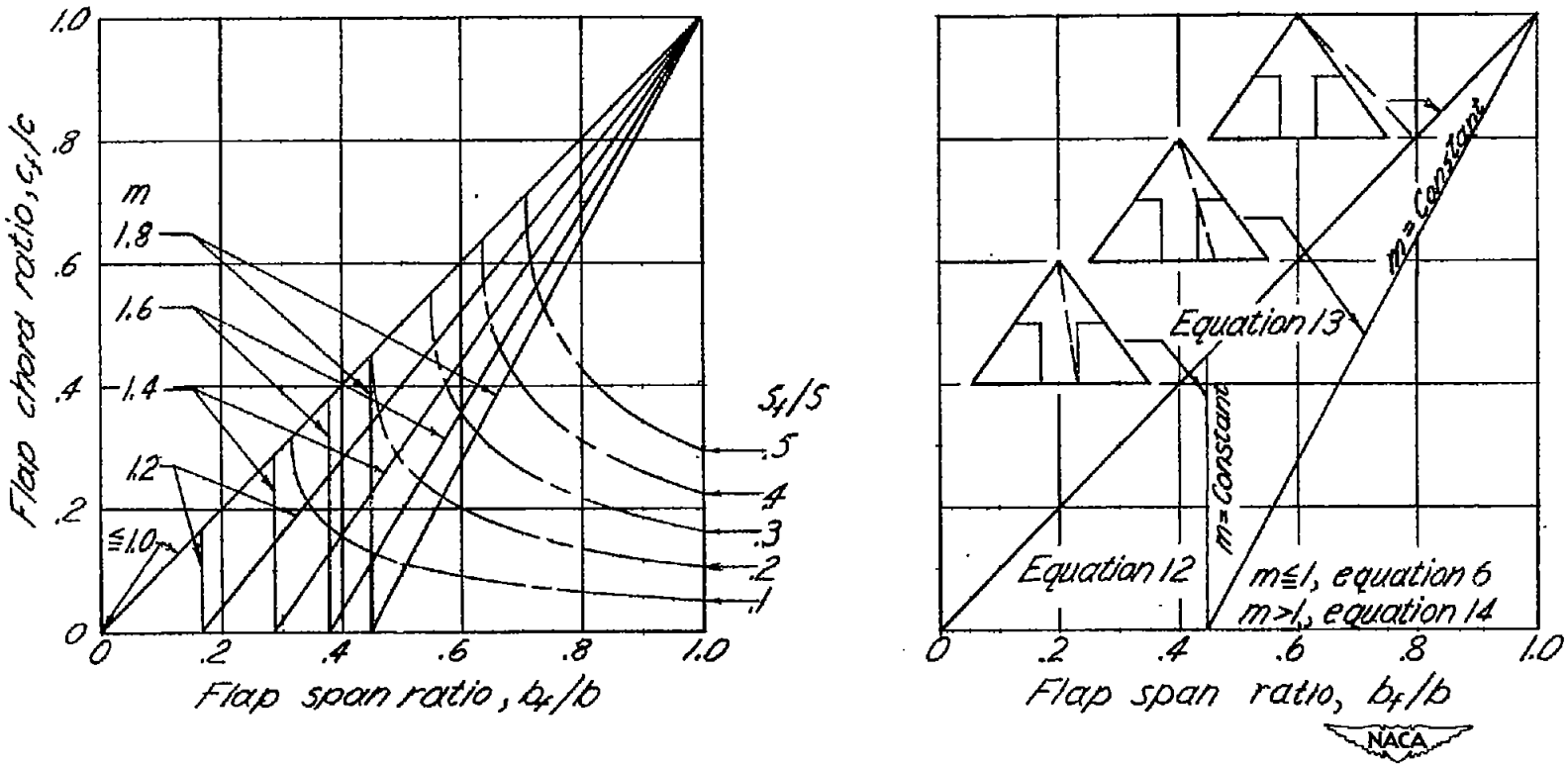

(c) C_{n_α} (equations 6, 12, 13, and 14).

Figure 5.- Concluded.

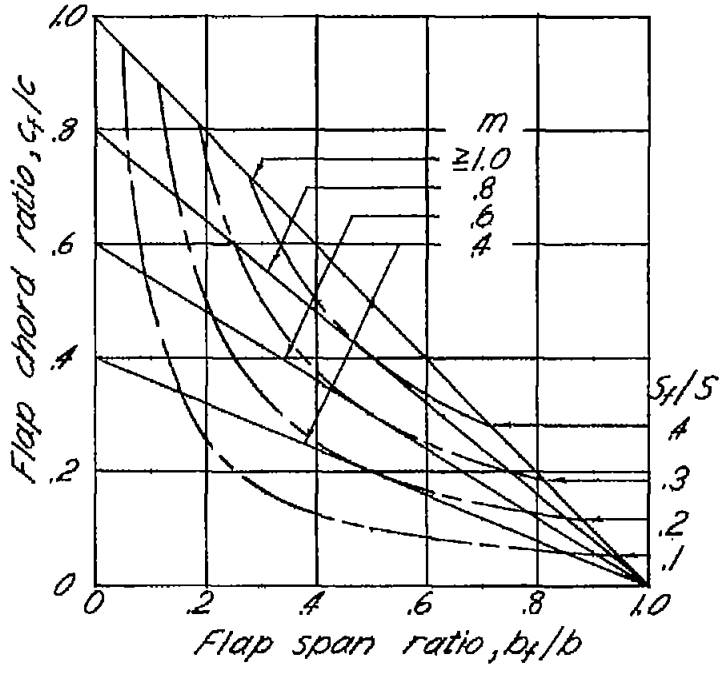

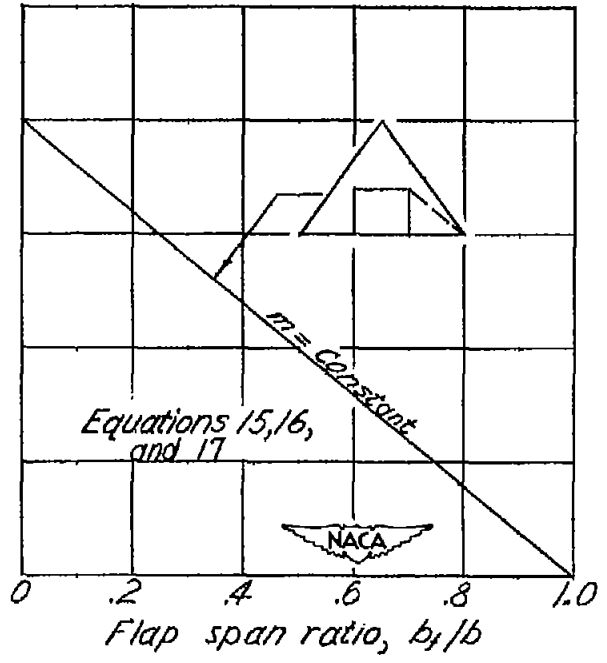

(a) C_{L_δ}, C_{l_δ}, $C_{m_{C_L}}$ (equations 15,16, and 17).

Figure 6.- Range of applicability of equations for inboard flaps.

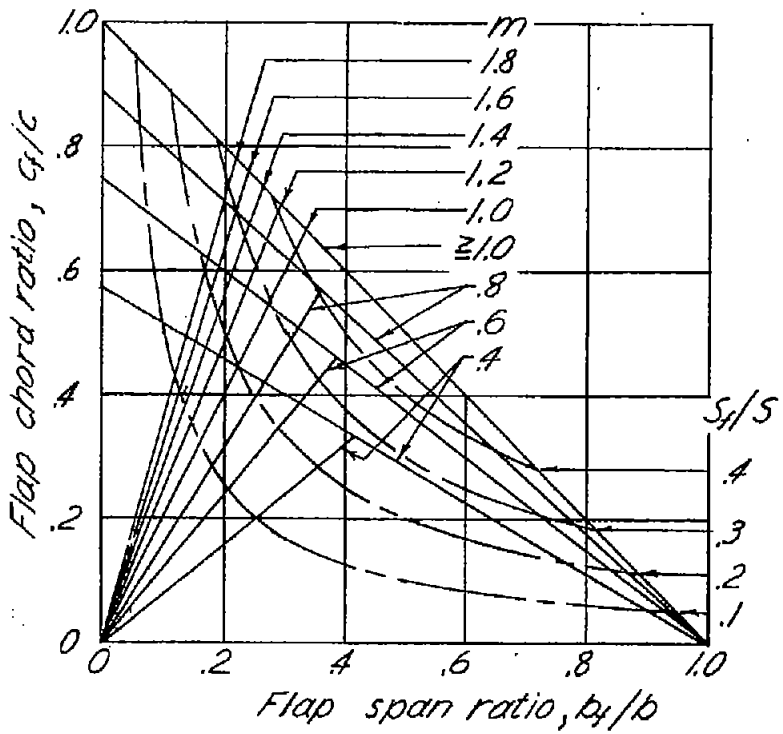

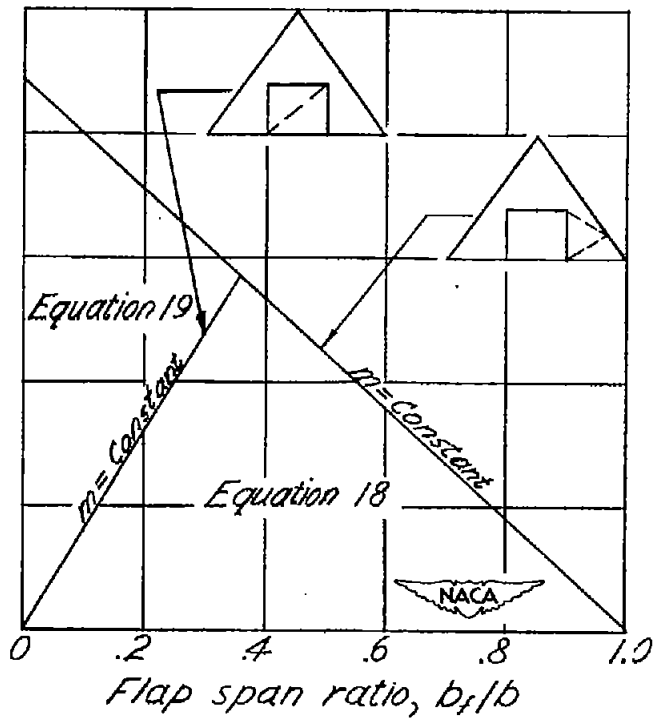

(b) C_{h_δ} (equations 18 and 19).

Figure 6.- Continued.

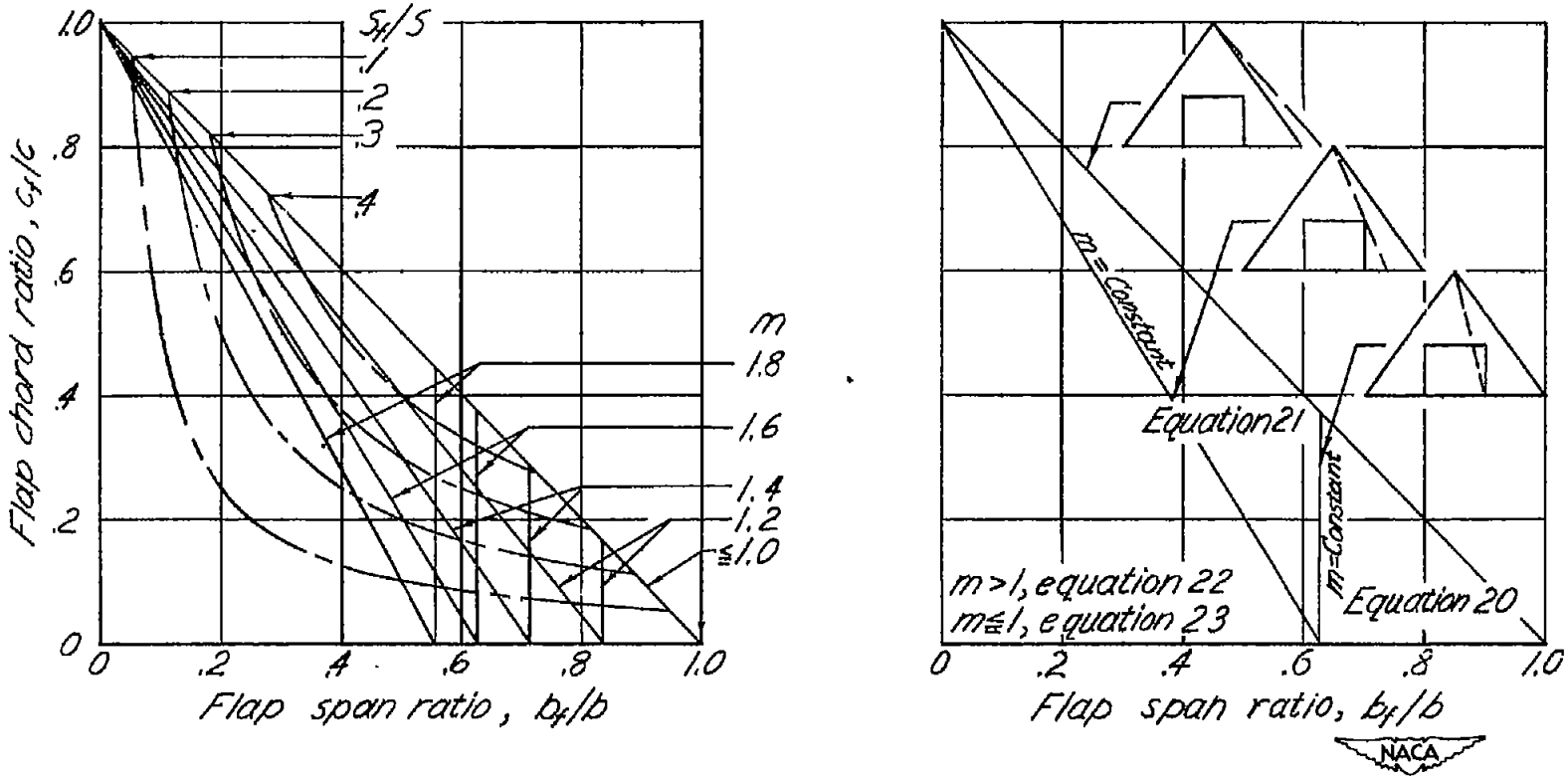

(c) C_{h_α} (equations 20, 21, 22, and 23).

Figure 6.- Concluded.

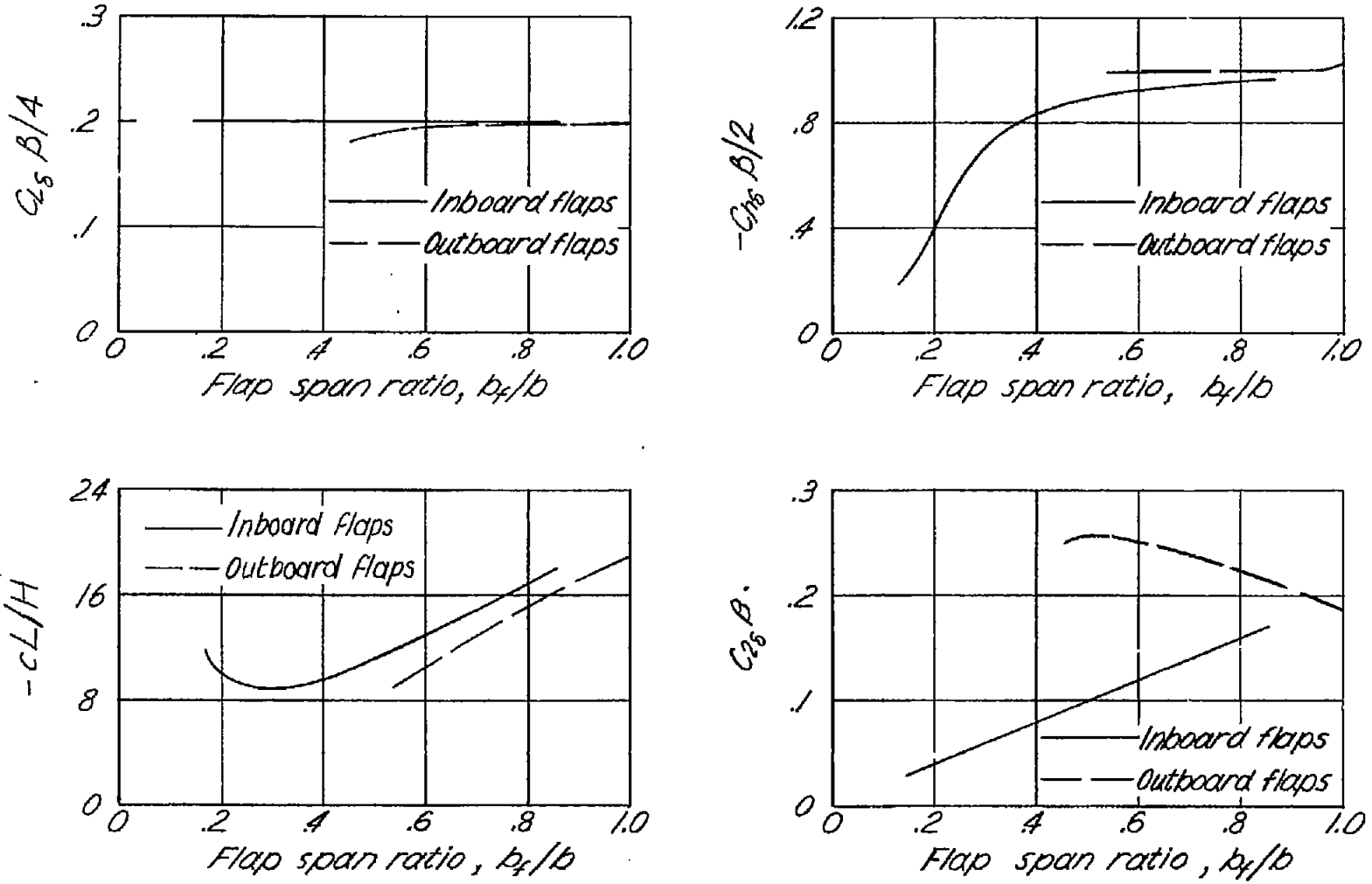

Figure 7.- Comparison of control-surface characteristics of inboard and outboard flaps. Flap area ratio $\frac{S_f}{S} = 0.2$; $m = 0.8$.

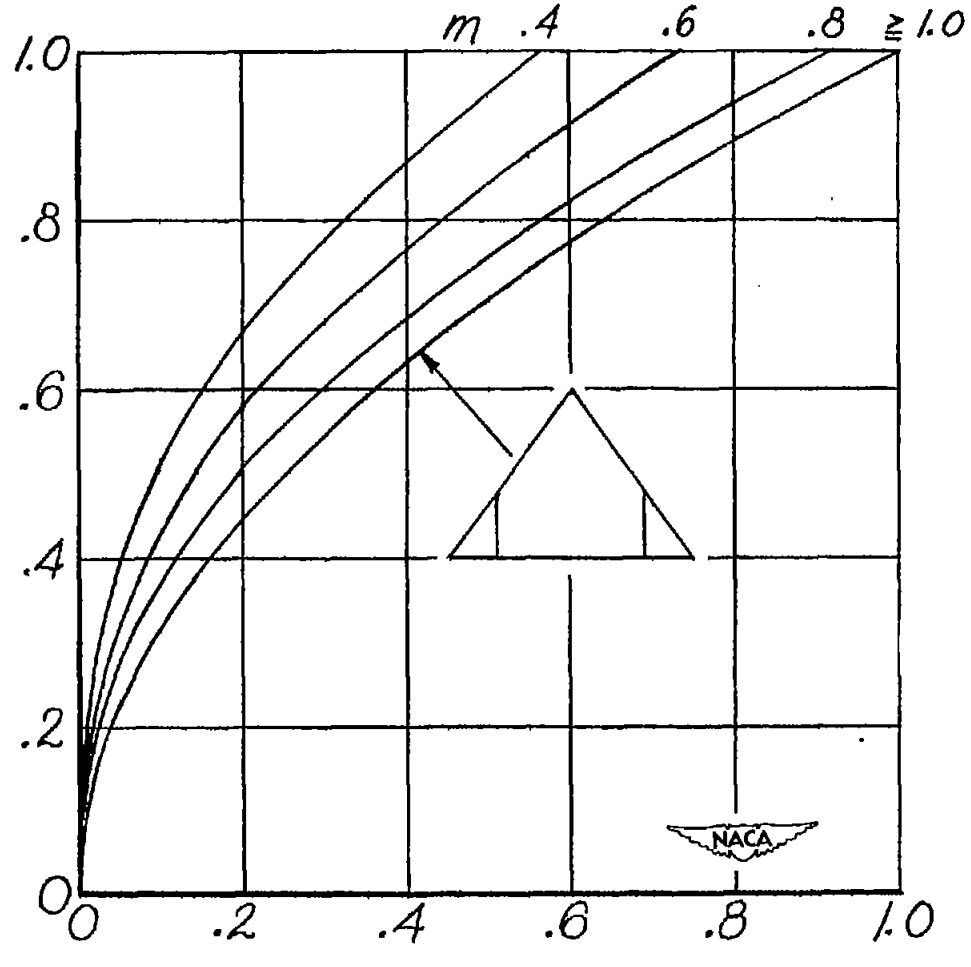

Figure 8.- Flap span ratio required for maximum rolling-moment effectiveness. Outboard flaps.

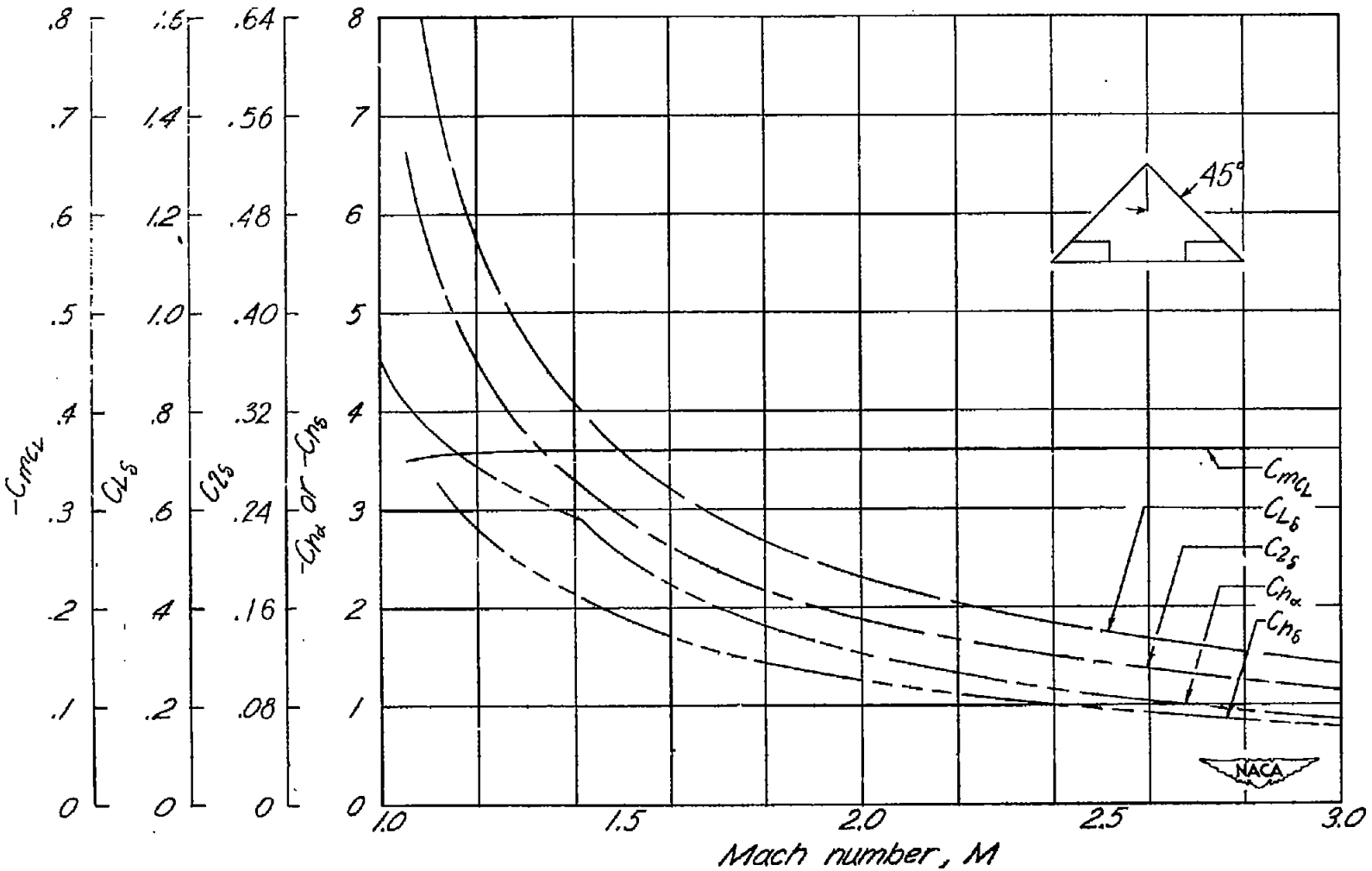

Figure 9.- Variation of control-surface characteristics with Mach number for outboard flaps. $\frac{S_f}{S} = 0.2$; $\frac{b_f}{b} = 0.6$; $\frac{c_f}{c} = 0.2$; $\epsilon = 45°$.

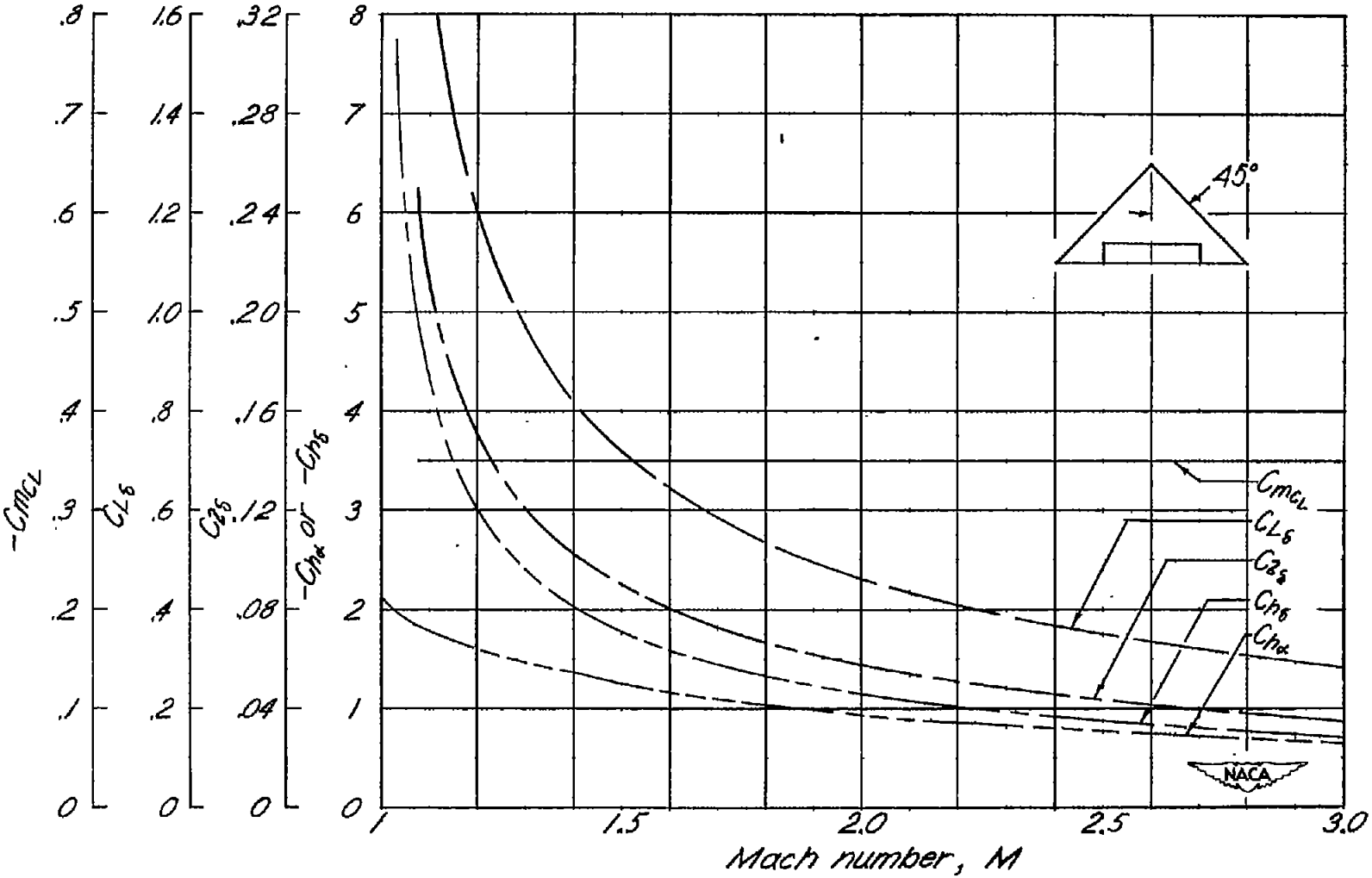

Figure 10.- Variation of control-surface characteristics with Mach number for inboard flaps. $\frac{S_f}{S} = 0.2$; $\frac{b_f}{b} = 0.5$; $\frac{c_f}{c} = 0.2$; $\epsilon = 45°$.

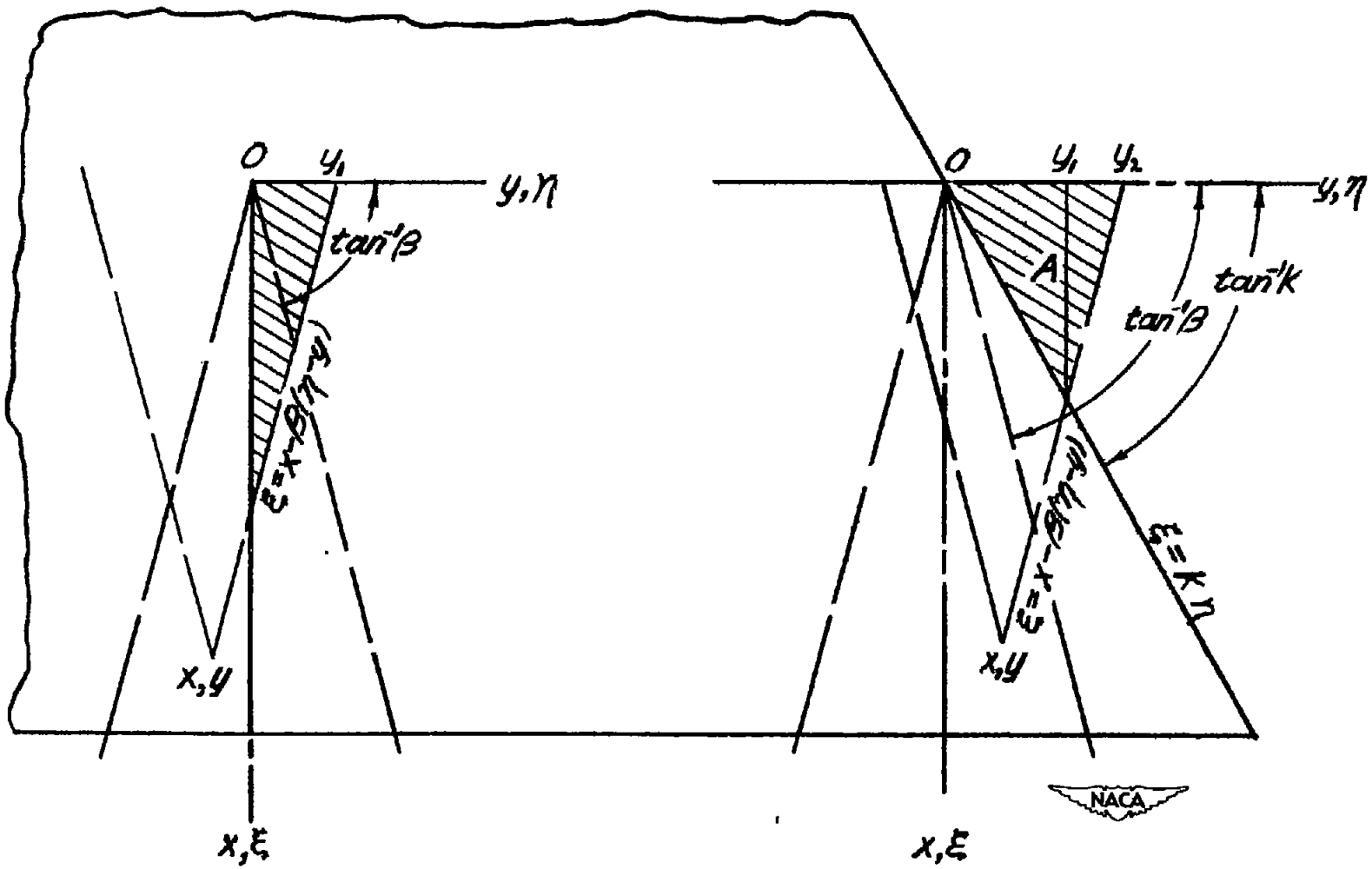

Figure 11.- Notation used in appendixes A and B.

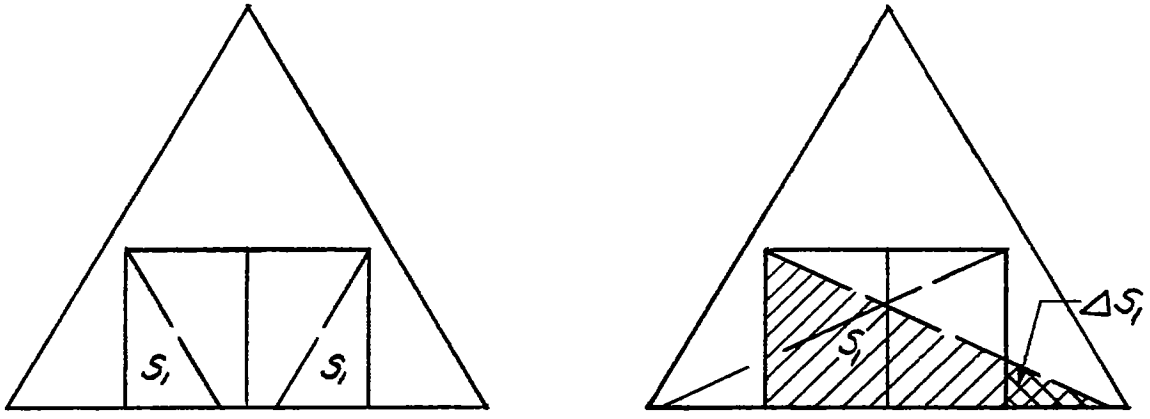

(a) Mach lines on flap. (b) Mach lines off flap.

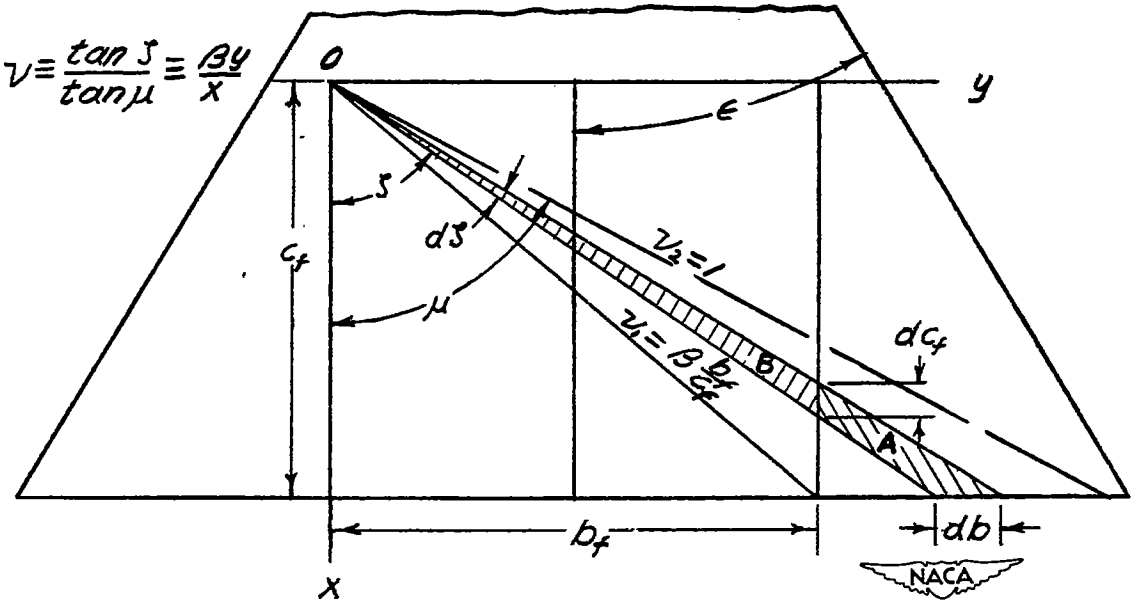

(c) Coordinate system and limits of integration for determining C_{h_δ}.

Figure 12.- Notation used in appendix D.